

Synthesis and Evaluation of a New Class of Cancer Chemotherapeutics Based on
Purine-like Extended Amidines

by

Evan Darzi

A Thesis Presented in Partial Fulfillment
of the Requirements for the Degree
Master of Science

Approved April 2011 by the
Graduate Supervisory Committee:

Edward Skibo, Chair
Ian Gould
Wilson Francisco

ARIZONA STATE UNIVERSITY

May 2011

ABSTRACT

A potential new class of cancer chemotherapeutic agents has been synthesized by varying the 2 position of a benzimidazole based extended amidine. Compounds 6-amino-2-chloromethyl-4-imino-1-(2-methansulfonyethyl)-5-methyl-*1H*-benzimidazole-7-one (1A) and 6-amino-2-hydroxypropyl-4-imino-1-(2-methansulfonyethyl)-5-methyl-*1H*-benzimidazole-7-one (1B) were assayed at the National Cancer Institute's (NCI) Developmental Therapeutic Program (DTP) and found to be cytotoxic at sub-micromolar concentrations, and have shown between a 100 and a 1000-fold increase in specificity towards lung, colon, CNS, and melanoma cell lines. These ATP mimics have been found to correlate with sequestosome 1 (SQSTM1), a protein implicated in drug resistance and cell survival in various cancer cell lines. Using the DTP COMPARE algorithm, compounds 1A and 1B were shown to correlate to each other at 77%, but failed to correlate with other benzimidazole based extended amidines previously synthesized in this laboratory suggesting they operate through a different biological mechanism.

DEDICATION

To my father Khalil Darzi, my mother Cynthia Avazpour, and Gabrielle Marie Macias for all their love and support.

ACKNOWLEDGMENTS

First, I would like to thank Dr. Skibo for taking a chance and giving me the opportunity to work in his lab. He taught me the skills necessary to succeed as a synthetic chemist, and taught me how important the student-mentor relationship is.

Second, I would like to thank Dr. Anne Jones for always being there to listen, even if it was not about chemistry, Dr. Mark Hayes for demystifying analytical chemistry, and Martha McDowell for being the best person at ASU to talk hockey with. Thank you to my committee for their guidance during my graduate program.

Finally, I would like to thank my parents for teaching me that no matter what your background or where you come from, hard work and dedication can get you anything you want.

TABLE OF CONTENTS

	Page
LIST OF TABLES	vi
LIST OF FIGURES	vii
LIST OF SCHEMES.....	ix
CHAPTER	
1 INTRODUCTION	1
Section 1.1 General Introduction	1
Section 1.2 Cancer Introduction.....	2
Section 1.3 Cancer Chemotherapy	4
Section 1.4 Modern Chemotherapy.....	8
Section 1.5 Extended Amidine Series	16
2 SYNTHESIS.....	25
Section 2.1 General Synthesis of 6-Amino-4-imino-1-(2- methansulfonyethyl)-5-methyl- <i>IH</i> -benzimidazole-7-ones.....	25
Section 2.2 Synthesis of 6-amino-2-chloromethyl-4-imino-1-(2- methansulfonyethyl)-5-methyl- <i>IH</i> -benzimidazole-7-one (1A)..	26
Section 2.3 Synthesis of 6-amino-2-hydroxypropyl-4-imino-1-(2- methansulfonyethyl)-5-methyl- <i>IH</i> -benzimidazole-7-one (1B) and 6-amino-4-imino-1-(2-methansulfonyethyl)-2- methansulfonypropyl-5-methyl- <i>IH</i> -benzimidazole-7-one (1C).	30
Section 2.4 Synthesis of 6-amino-4-imino-1-(2- methansulfonyethyl)-5-methyl- <i>IH</i> -benzimidazole-7-one (1D)..	33

	Page
Section 2.5 Synthesis of 1,5-dimethyl-1 <i>H</i> -benzimidazole-2-methanamine (15)	35
3 RESULTS AND DISCUSSION	36
Section 3.1 NCI Cell Line Studies	36
Section 3.2 Potency of Compounds 1A and 1B	36
Section 3.3 Specificity of Compounds 1A and 1B	38
Section 3.4 DTP COMPARE.....	41
4 CONCLUSION.....	48
5 EXPERIMENTAL	49
Section 5.1 General Experimental.....	49
Section 5.2 Synthesis of Listed Compounds.....	49
REFERENCES	62

LIST OF TABLES

Table		Page
1.	Cell Lines by Panel	17
2.	Matrix Compare of 1A, 1B, 736296 and 732650	43
3.	Molecular Target Compare Matrix	44
4.	Back Correlation of SQSTM1	46

LIST OF FIGURES

Figure		Page
1.	Extended Amidine Moiety	1
2.	Iminoquinone Pharmacophore	1
3.	Indirubin	5
4.	Salvarsan	6
5.	Nitrogen Mustard	6
6.	Folic Acid, Methotrexate, and Aminopterin	7
7.	The Cell Cycle	8
8.	Mitochondrial Apoptosis	10
9.	Death Receptor Pathway	11
10.	Daunorubicin	12
11.	Dacarbazine	13
12.	Mechlorethamine Mechanism of Bisalkylation	13
13.	Taxol	14
14.	Estrone	14
15.	Bortezomib and Fludarabine	16
16.	Wakayin and Makaluvamine D.....	18
17.	Dose Response Curve	18
18.	Mean Graph Example	19
19.	Wortmannin	20
20.	Extended Amidine Pharmacophore	21

Figure	Page
21. Electrostatic Potential Map of the Extended Amidine Core and Adenine	22
22. SL0101	22
23. Synthetic Targets	23
24. Dose Response Data for Compound 1A and 1B	36
25. Mean Graph of Compound 1A	38
26. Mean Graph of Compound 1B	39
27. Triangular Correlation	42
28. Compounds 736296 and 732650	43
29. Mean Graph Data of 1A Over SQSM1 and 1B Over SQSTM1 by Cancer Panel	44
30. Triangular Correlation of 1A/1B, SQSTM1, and 656909.....	46

LIST OF SCHEMES

Schemes		Page
1.	General Synthesis of Extended Amidines	26
2.	Synthesis of 4-(2-hydroxyethylamino)-3-nitrotoluene (3)	26
3.	Synthesis of 5-methyl-1-(2-oxyethyl)-2-oxymethyl-benzimidazole (4)	27
4.	Synthesis of 4,6-dinitro-5-methyl-1-(2-nitrooxyethyl)-2- nitrooxymethyl- <i>IH</i> -benzimidazole (5)	27
5.	Synthesis of 6-amino-4-imino-1-(2-hydroxyethyl)-2-hydroxymethyl-5- methyl- <i>IH</i> -benzimidazole-7-one (6)	27
6.	Mechanism of Fremy Oxidation	28
7.	Synthesis of 6-amino-2-chloromethyl-4-imino-1-(2- methansulfonyethyl)-5-methyl- <i>IH</i> -benzimidazole-7-one (1A) ..	28
8.	Regioselective Substitution	29
9.	Synthesis of 5-methyl-1-(2-oxyethyl)-2-oxypropyl-benzimidazole (7)	30
10.	Synthesis of 4,6-dinitro-5-methyl-1-(2-nitrooxyethyl)-2- nitrooxypropyl- <i>IH</i> -benzimidazole (8)	31
11.	Synthesis of 6-amino-4-imino-1-(2-hydroxyethyl)-2-hydroxypropyl-5- methyl- <i>IH</i> -benzimidazole-7-one (9)	31
12.	Synthesis of 6-amino-2-hydroxypropyl-4-imino-1-(2- methansulfonyethyl)-5-methyl- <i>IH</i> -benzimidazole-7-one (1B) and	

Schemes	Page
6-amino-4-imino-1-(2-methansulfonyethyl)-2-methansulfonypropyl- 5-methyl- <i>IH</i> -benzimidazole-7-one (1C)	32
13. Regioselectivity of Sulfonation Due to Anchimeric Assistance	33
14. Synthesis of 1-(2-Hydroxyethyl)-5-methylbenzimidazole (10)	33
15. Synthesis of 4,6-dinitro-5-methyl-1-(2-nitrooxyethyl)- <i>IH</i> - benzimidazole (11)	33
16. Synthesis of 6-amino-4-imino-1-(2-hydroxyethyl)-5-methyl- <i>IH</i> - benzimidazole-7-one (12)	34
17. Synthesis of 6-amino-4-imino-1-(2-methansulfonyethyl)-5-methyl- <i>IH</i> -benzimidazole-7-one (1A)	34
18. Synthesis of N,3-dimethyl-2-aminoaniline (14)	35
19. Synthesis of 1,5-dimethyl- <i>IH</i> -benzimidazole-2-methanamine (15) .	35

Chapter 1

INTRODUCTION

1.1 General Introduction

The natural product base extended amidine moiety (figure 1) and iminoquinone pharmacophore (figure 2) have previously been shown by this lab to be selectively cytotoxic against melanoma, lung and colon cancer (LaBarbera & Skibo, 2005) (Hoang, LaBarbera, Mohammed, Chris, & Skibo, 2007).

Figure 1: Extended Amidine Moiety

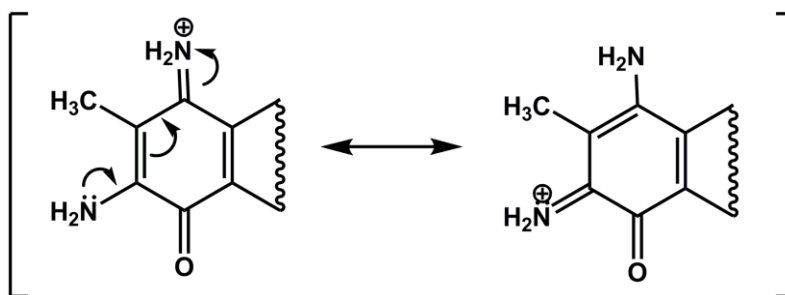
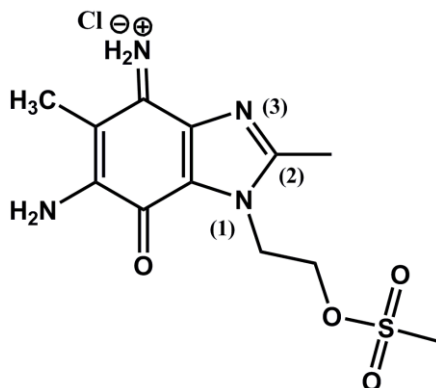


Figure 2: Iminoquinone Pharmacophore



The COMPARE algorithm at the National Cancer Institute (NCI), which correlates cell line data to a database of mRNA drug targets and other chemotherapeutic agents, suggests they are selective kinase inhibitors in the AKT apoptosis pathway. A new class of iminoquinones, with substitution at the 2

position of the imidazole, has been designed to increase activity and improve specificity in cancer cells. The design methodology will be presented shortly, but in order to understand how this new class of compounds was created it is necessary to understand why.

1.2 Cancer Introduction

In 2010 there were 1,529,560 new cases of cancer and 569,490 cancer related deaths in the United States alone (American Cancer Society, 20). At the most basic level, cancer can be thought of as the ratio of cell proliferation divided by cell death and as this ratio becomes larger, cancer becomes more prevalent (Hickman & Tritton, 1993). This is an obvious oversimplification as there are many factors shown to lead to the various types of cancer and the subset of factors responsible for their progression. Although these biochemical factors can vary according to cancer type, cancer can be divided into four basic categories, Carcinomas, Lymphomas, Leukemia, and Sarcomas. The first, and most common accounting for nearly 90% of all cancers, are Carcinomas, these are cancers that originate in the skin, lungs, breast, and other organs and glands. The second, Lymphomas, are cancers that originate from lymphocytes, the third, Leukemia, are cancers of blood cells. The final and rarest are the Sarcomas which originate in bone, muscle, fat, or cartilage. Cancers are also categorized by the location in the body where they are first observed for example, melanoma is defined as a cancer originating in the epidermis (Herlyn, 1993).

Tumors are classified into two categories, benign or malignant. The first is defined as a mild, non progressive tumor that is rarely life threatening, while

the latter is more aggressive and has the ability to spread to other tissue and organs through a process known as metastasis. Malignant tumors are the more dangerous of the two and can vary mechanistically in how and where they metastasize (Barnhill, 1995). There are four general causes of cancer: 1) Genetic background; 2) viruses; 3) radiation; and 4) chemical carcinogens.

There are over fifty types of cancer thought to be hereditary, meaning there is a genetic predisposition to specific types of cancer. In 2010 it was reported that between five and ten percent of breast cancer fatalities and fifteen to twenty percent of new breast cancer cases had a history of familial breast cancer (American Cancer Society,). There is a one in ten chance that the average woman will develop breast cancer, but this risk is doubled if the woman has a relative who was been diagnosed with it.

Radiation including UV rays, X-rays, and gamma rays from natural and manmade sources can cause cancer through DNA fragmentation, pyrimidine dimer formation, and oncogene activation. UVB, for example, is responsible for activation of thirty nine percent of N-ras oncogenes in melanoma (Hocker & Tsao, 2007). UVB is also responsible for the photo[2+2] cycloaddition of thymine bases in DNA, when nucleotide excision repair is lacking, these dimers may lead to the formation of melanomas (Hocker & Tsao, 2007).

Viruses also play a role in cancer development, these oncogenic viruses insert their genetic information into the host chromosomal DNA in proximity to a proto-oncogene. The human papilloma virus, for example, has been reported to account for more than eighty percent of cervical cancers, and has recently been

shown to correlate to oro-pharynx and esophagus cancers in both men and women. This is just one of many oncogenic viruses known, other important examples include the Epstein-Barr virus shown to be responsible for Burkitt's lymphomas, hepatitis B shown to correlate to liver cancers, and the human T-cell leukemia virus (Shukla et al., 2009).

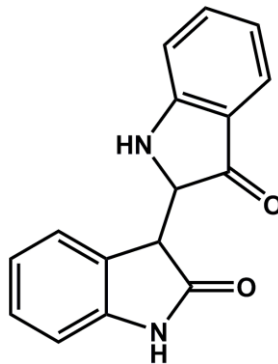
Permanent mutations in DNA caused by chemical carcinogens can also lead to various cancers. The carcinogenesis begins with an initiation stage where exposure to a carcinogen induces a rapid irreversible mutation that renders the cell immortal, but not tumorigenic. During the promotion stage, prolonged exposure to non-genotoxic compounds disrupts this cell's environment resulting in proliferation and tumorigenesis (Trosko, 2003). For example, cigarette smoke, which is reported to be responsible for eighty-seven percent of lung cancer deaths, contains over 3,500 compounds and 10^{14} - 10^{16} free radicals per puff. Many of these compounds along with radical-induced reactive oxygen species (ROS) have individually been shown to act as initiators or promoters of cancer, and in some cases act as both (Li, Zhou, Chen, Luo, & Zhao, 2011).

Although it is impossible to avoid all of the risk factors associated with cancer, there are several ways an individual can limit their susceptibility including avoiding known carcinogens like cigarette smoke, habitual use of sunscreen to limit UVB radiation exposure, and being aware of how carcinogenic viruses like HPV can be avoided.

1.3 Cancer Chemotherapy

Chemotherapy is the treatment of an ailment using chemicals, when considering various natural products such as indirubin (figure 3), derived from the Chinese *Isatis tinctoria*, the history of chemotherapy dates back to antiquity (Wilson, Gisvold, Block, & Beale, 2004).

Figure 3: Indirubin

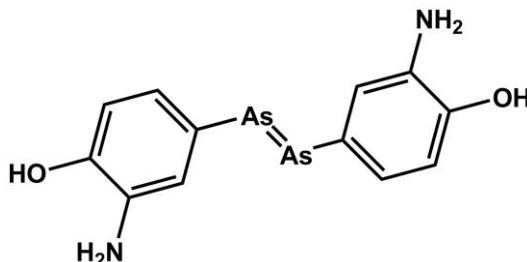


A brief history of rational and random drug design, along with the model used to test these compounds is important in understanding the methodology used to create the extended amidine series.

Modern chemotherapy began in the 1890's after three major scientific findings, the discovery of penetrating radiation by Dr. Roentgen in 1895, the discovery that the removal of the ovaries halted the progression of breast cancer by Dr. Beatson in 1896, and finally the discovery that patient immunization using sterilized bacterial extracts caused a regression in lymphomas and sarcomas by Dr. Coley in 1898. These findings had two important implications, first, they showed that external measures could be exploited to treat cancers, and second, they suggested that small molecules could be used in the treatment of cancer and other infectious diseases (Baguley & Kerr, 2002). By the early 1900's Paul

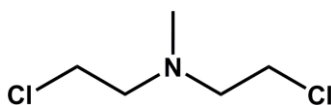
Ehrlich had used these concepts to treat syphilis using a dye derived prodrug Salvarsan (figure 4), Ehrlich is also credited with coining the term chemotherapy.

Figure 4: Salvarsan



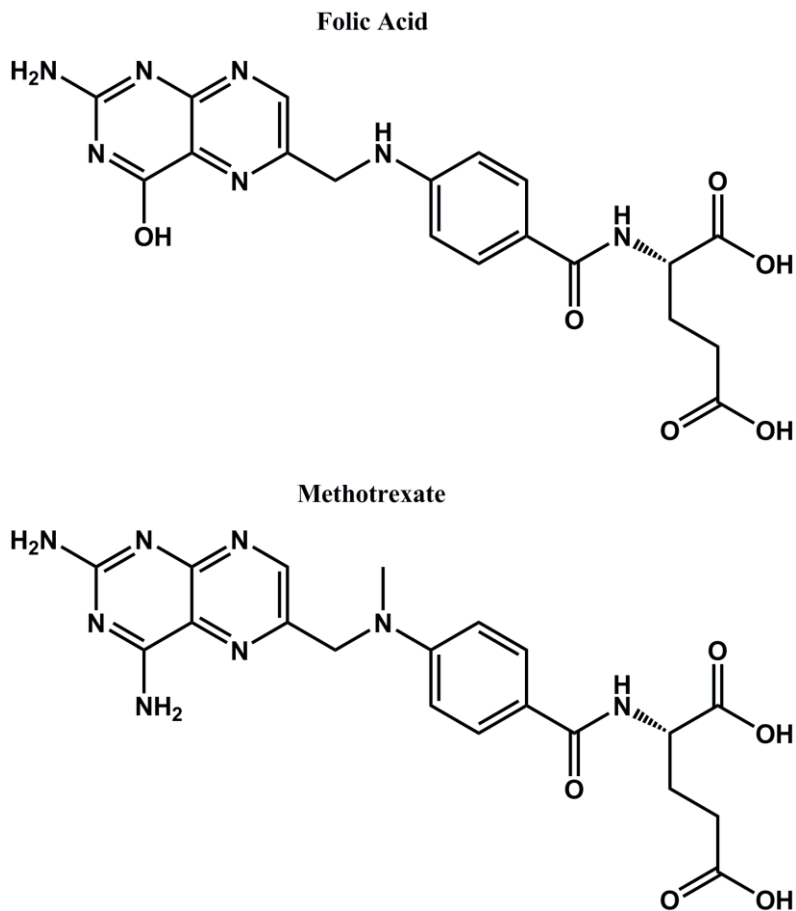
Around the same time another scientific innovation opened the doorway for chemotherapeutic screening, Dr. George Clowes developed the first *in vivo* model using transplantable rodent tumors (DeVita & Chu, 2008). This rodent model provided not only a method to test potential cancer therapeutics, but also spurred efforts to find an optimal model for to understand cancer. The first widely used synthetic chemotherapeutic agent was discovered like many great scientific findings, by accident. A large quantity of sulfur mustard gas was released from a damaged American war ship in the bombing of Bari Harbor during World War II. Doctors noticed that the lymph nodes and bone marrow had been significantly depleted in soldiers exposed to the sulfur mustard gas. This led to the development of nitrogen mustard (figure 5) treatment of non-Hodgkin's lymphoma in 1943 by Dr. Milton Winternitz of Yale University who used transplanted lymphoma tumors in mice as a model (DeVita & Chu, 2008).

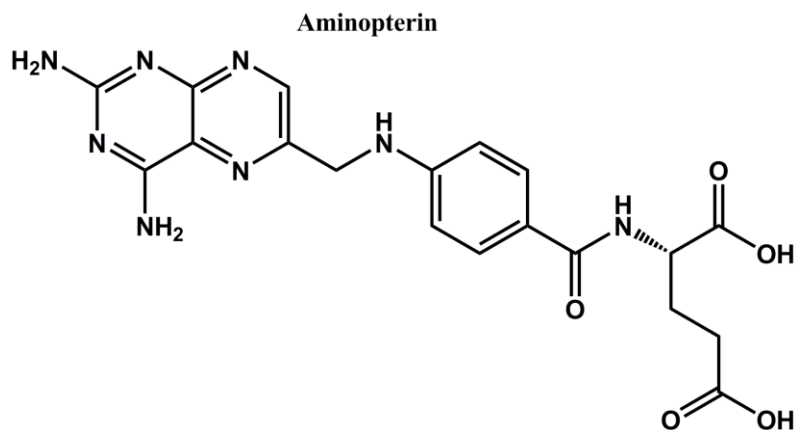
Figure 5: Nitrogen Mustard



The final important breakthrough that helped define rational drug design came from Dr. Sidney Farber. Prior to World War II research had shown that folic acid was necessary to sustain regular bone marrow growth meanwhile Dr. Farber, a pathologist interested in leukemia, began testing the effects of folic acid (figure 6) on acute lymphoblastic leukemia. He found that an increase in folic acid actually exacerbated cell growth, he then partnered with Dr. Harriet Kille to develop several folic acid analogues. By 1947 Dr. Farber had found two effective anti folate drugs, aminopterin and methotrexate (figure 6), that put leukemia into remission (DeVita & Chu, 2008).

Figure 6: Folic Acid, Methotrexate, and Aminopterin





Although there were several breakthroughs in cancer chemotherapy after this point in history, these aforementioned findings set the ground work for all rational and random drug development and screening.

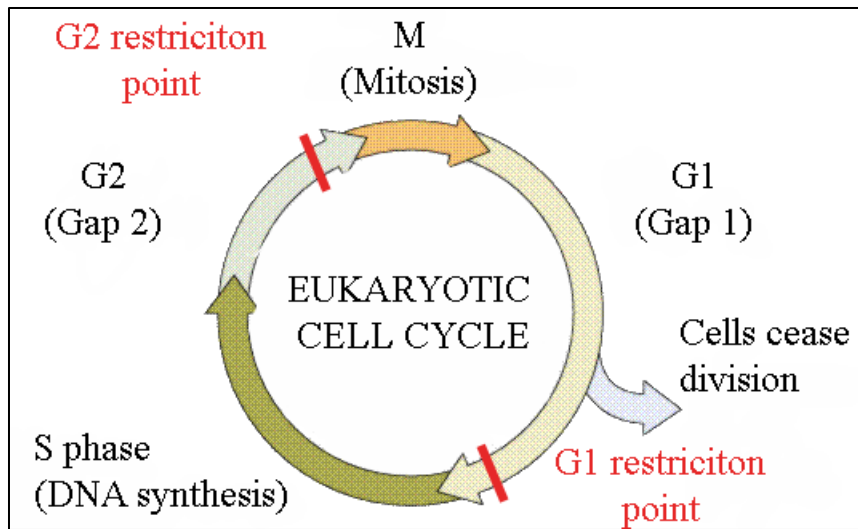
1.4 Modern Chemotherapy

Modern chemotherapeutic is best described at a biochemical level and currently, two broad exploitable pathways are used to understand and treat cancer;

1) Cell cycle and cell cycle checkpoints including growth factors and signal transduction; and 2) Cell death, otherwise known as apoptosis. As each is explained keep in mind the most basic definition of cancer in terms of cell proliferation and cell death.

The cell cycle can be thought of as a clock that represents the growth, proliferation, and death of any cell (figure 7).

Figure 7. The Cell Cycle



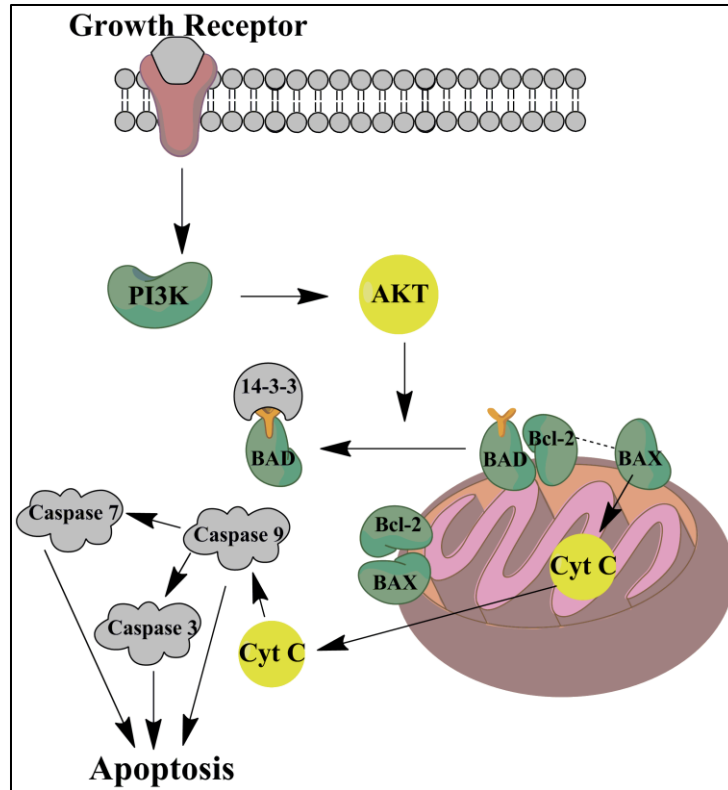
The cycle begins in the G₁ phase in which a cell synthesizes the necessary organelles to survive and grows to its normal size, this phase is held in a non dividing state by a restriction point of biochemical growth pathways that when activated allow the progression from the G₁ phase into the S phase responsible for DNA replication. The G₁ restriction point is regulated by G₁ cyclin-dependent kinases (CDK) which first require binding of the necessary cyclin protein followed by phosphorylation by a CDK activating kinase (CAK) in order to promote passage into the S phase. During the S phase, DNA is checked for damage, repaired, and replicated in preparation for the G₂ phase. The G₂ phase occurs directly after the S phase and is responsible for synthesizing proteins necessary for mitosis and is used as a restriction point to regulate DNA damage due to genotoxic stress. This restriction point is tightly regulated by protein 53 (p53), if DNA damage is sensed p53 is able to arrest the cell in the G₂ phase while the damage is repaired, or if the damage is severe enough, it can signal an

apoptosis cascade resulting in cell destruction (Baguley & Kerr, 2002; Herlyn, 1993; Hickman & Tritton, 1993).

Apoptosis can be defined as the internal regulation of cell death, not to be confused with necrosis which is cell death in response to tissue injury and inflammation (Hickman & Tritton, 1993). Apoptosis is tightly regulated by two main groups of enzyme cascades; 1) the mitochondrial pathway; and 2) the death-receptor-dependent pathway.

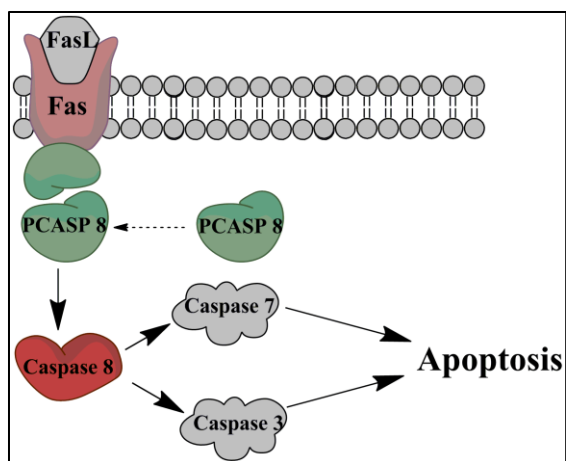
The mitochondrial pathway begins at the surface of the cell, here transmembrane G-proteins can activate phosphoinositide 3-kinase (PI3K) which can activate the survival protein AKT1. Once activated, this kinase is able to phosphorylate Bcl-2 associated death (BAD) which when phosphorylated is sequestered in the cytosolic 14-3-3 family proteins. When BAD is not phosphorylated it migrates to the surface of the mitochondria where it heterodimerizes with Bcl-2, this dimerization releases Bcl-2 associated X protein (BAX). BAX and several homologues of BAX are responsible for mitochondrial dysfunction followed by the release of cytochrome c into the cytosol when not associated with the survival protein Bcl-2. Cytochrome c can then activate caspase 9, a cysteine protease, followed by caspase 3 and 7 which are responsible for complete cellular destruction (figure 6) (Chao & Korsmeyer, 1998; Henshall et al., 2002; Kitada et al., 1998; Lopez-Bergami & Fitchman, 2008; Qin, Xin, Sitailo, Denning, & Nickoloff, 2006; Reed, 1994).

Figure 8: Mitochondrial Apoptosis



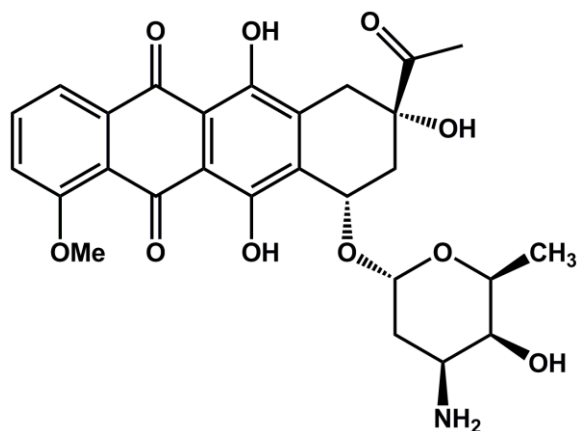
The death-receptor-dependant pathway begins when the death ligand FasL binds to the transmembrane death receptor Fas, this induces a conformational change on the cytosolic side of the membrane and formation of the death domain (DD). Once formed, it is able to bind and activate pro-caspase 8, this activated caspase is then released into the cytosol where it can directly activate caspase 3 and 7 which rapidly degrades the cell (figure 9) (Baguley & Kerr, 2002; Lopez-Bergami & Fitchman, 2008).

Figure 9: Death Receptor Pathway



Several mutations in both the cell cycle and apoptosis are necessary for cancers to overcome the many checks and balances that regulate cell life and death. Different drug therapies are necessary for each type of cancer due to the variation in mutations (Baguley & Kerr, 2002). Cancer therapeutics can be broken down into six classes based on their mechanism of action; 1) Antitumor antibiotics, such as daunorubicin (figure 10) for example, act by intercalating DNA. By intercalating DNA in the minor or major groove, DNA replication machinery is not able to function and thus cell proliferation is halted (Hickman & Tritton, 1993).

Figure 10: Daunorubicin



2) Alkylating agents, such as dacarbazine (figure 11), act by covalent modification of DNA typically at the nucleophilic N-7 of guanine. Agents with multiple alkylation sites, like nitrogen mustards (figure 5), are able to cross link DNA (figure 12), both methylation and DNA cross linking can lead to depurination followed by DNA strand scission or miscoding leading to guanine mispairing with thymine instead of cytosine. This DNA damage can be sensed at cell cycle checkpoints which then signal the cell for apoptosis (Hickman & Tritton, 1993; Rümke, 1990) (Wilson et al., 2004).

Figure 11: Dacarbazine

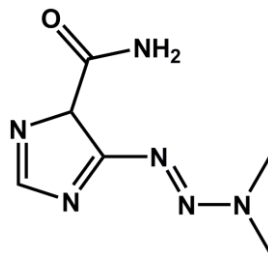
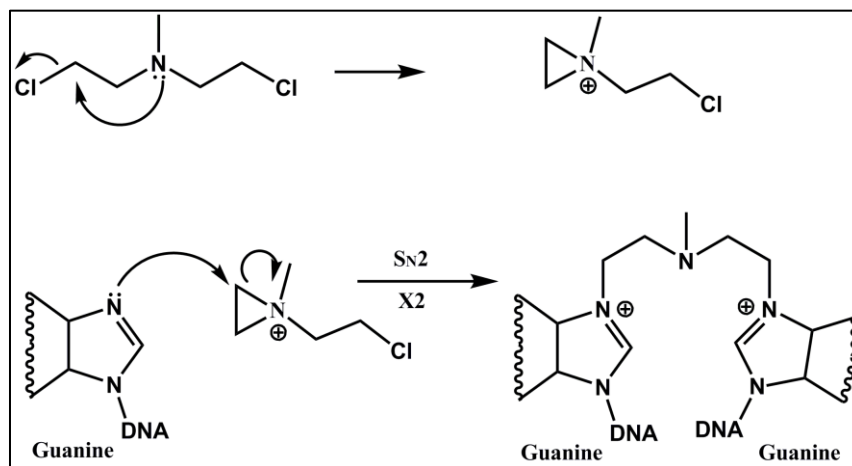


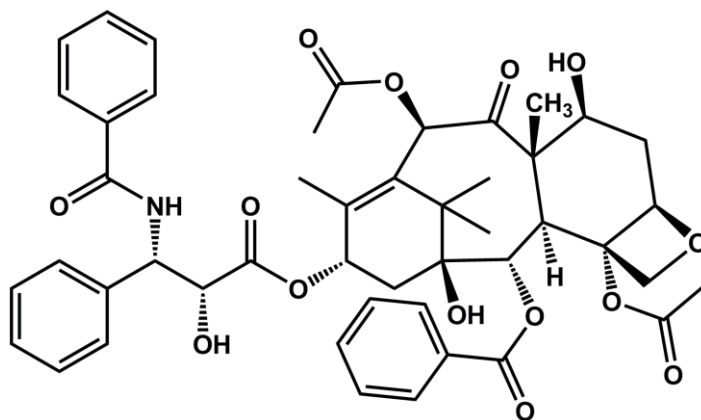
Figure 12: Mechlorethamine Mechanism of Bisalkylation



3) Antimitotic agents, such as taxol (figure 13), interfere with the molecular machinery used during mitosis. Taxol is used to stabilize microtubule polymers

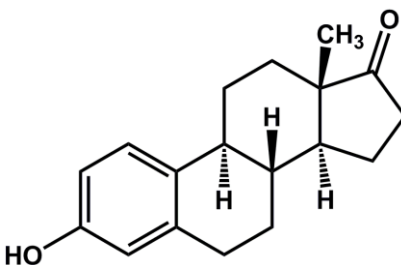
during mitosis which interferes with mitotic spindles, this arrests the cell at the mitosis checkpoint leading to a return to the G1 phase or signaling leading to apoptosis (Baguley & Kerr, 2002; Wilson et al., 2004).

Figure 13: Taxol



4) Hormones and hormone inhibitors are used to alter the endocrine system based on certain cancers sensitivity to hormones, estrogen (figure 14) for example is used to suppress testosterone production in patients with prostate cancer (Hickman & Tritton, 1993).

Figure 14: Estrone



5) Monoclonal antibodies are used to specifically target and flag cancer cells for destruction by the immune system or by delivery of a cytotoxic agent.

Tositumomab, for example, is covalently bound to the radio isotope iodine-131

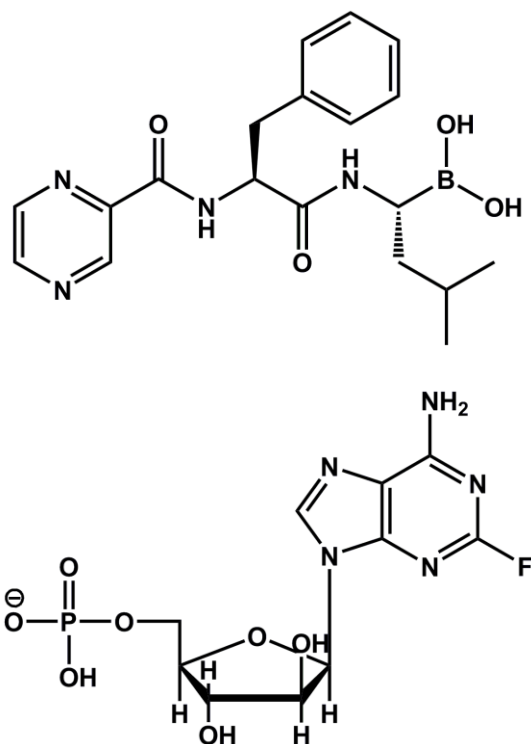
and specifically targets follicular lymphoma, this allows site specific radiation treatment to limit the exposure of healthy tissue (Baguley & Kerr, 2002).

6) The final and most important class of cancer chemotherapeutic agents in terms of this research are the anti metabolites. Anti metabolites are drugs that interfere with enzyme pathways and/or nucleotide synthesis. The folic acid (figure 6) analog methotrexate (figure 6), for example, has over a one thousand fold higher affinity for dihydrofolate reductase than its natural substrate folic acid, which is necessary for the biosynthesis of the nucleoside thymidine. Without the ability to synthesize thymidine, DNA synthesis halts and cancer cells starve (Baguley & Kerr, 2002; DeVita & Chu, 2008; Hickman & Tritton, 1993).

Due to the variation in mutations between cancer types, different drug combinations are necessary to target the faulty pathway according to histological specificity. A synergistic effect is found when multiple pathways are targeted, for example, the combination of pro apoptotic Bcl-2 enzyme NOXA activation using bortezomib, and fludarabine used to block cell survival protein Mcl-1 (Qin et al., 2006) (figure 15). Bortezomib and fludarabine were found to kill 11 and 35 percent of melanoma (Berger et al., 2011) cells respectively at a 10 μ M concentrations, when used in combination up to 60 percent of the cells were killed using 5 μ M concentrations of each (Qin et al., 2006). This suggests that drugs that can specifically target an enzyme or pathway implicated in cancer could be used in combination to eliminate cancer from the host body while limiting the destruction of healthy tissue (Berger et al., 2011). The extended amidines were

investigated for their potential to selectively target kinases in the apoptosis pathway.

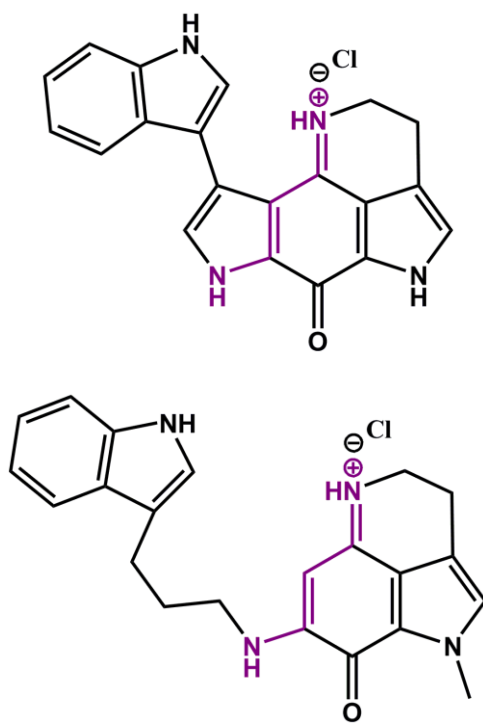
Figure 15: Bortezomib and Fludarabine



1.5 Extended Amidine Series

The extended amidine moiety (figure 1) was studied in our lab in an attempt to simplify the pharmacophore for several previously studied alkaloid pigments isolated from marine sponges and to increase their activity *in vitro*. These pigments, including makaluvamines and wakayins (figure 16), were previously shown to have a wide range of cytotoxic cellular targets such as topoisomerase I and II poisoning (Carney, Scheuer, & Kelly-Borges, 1993; Copp, Ireland, & Barrows, 1991). The extended amidine resonance, highlighted in purple, is responsible for the brilliant pigmentation in these compounds.

Figure 16. Wakayin and Makaluvamine D



In order to isolate the simplest pharmacophore of these pigments, several analogs were synthesized and screened against the *in vitro* 60 cell line at the National Cancer Institute (NCI) to determine the structural motifs that are required for cytotoxicity (Boyd & Paull, 1995). The NCI 60 *in vitro* cell line data gives several important pieces of data used to analyze the potency, specificity, and potentially the target of each compound screened.

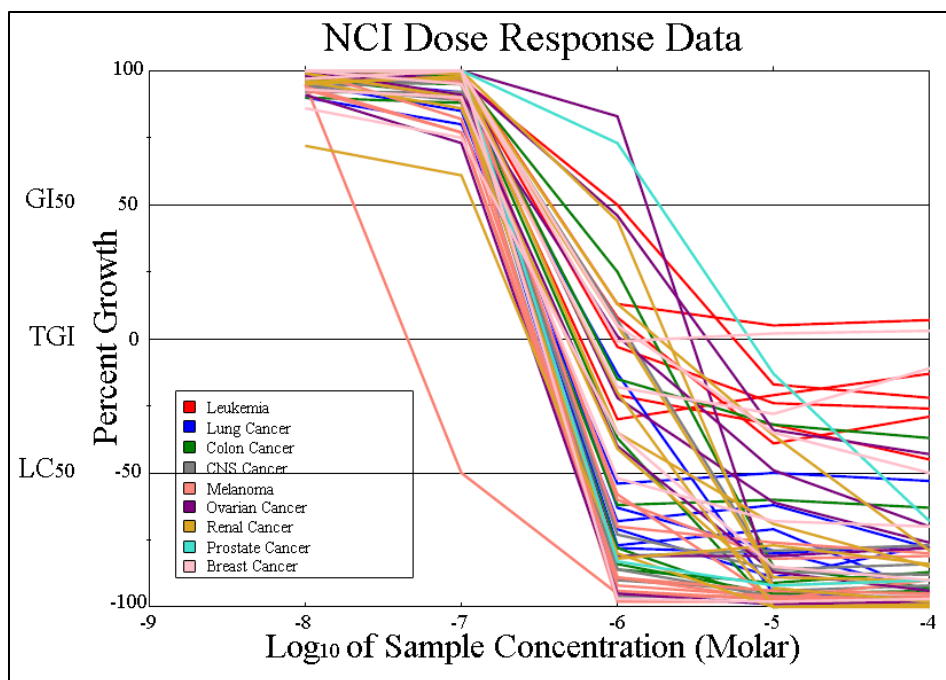
The 60 cell line is composed of 60 of the most common and culturable cancer cells lines summarized in table 1.

Table 1. Cell Lines by Panel

Cell Line by Panel Type			
Lung	Melanoma	Renal	Ovarian
A549/ATCC	LOXIMVI	786-0	IGROV1
EKVX	MALME-3M	A498	OVCAR-3
HOP-62	M14	ACHN	OVCAR-4
HOP-92	MDA-MB-435	CAKI-1	OVCAR-5
NCI-H226	SK-MEL-28	RXF393	OVCAR-8
NCI-H23	SK-MEL-5	SN12C	NCI/ADR-RES
NCI-H322M	UACC-257	TK-10	SK-OV-3
NCI-H460	UACC-62	UO-31	
NCI-H522			
Colon	Leukemia	CNS	Breast
COLO205	CCRF-CEM	SF-268	MCF7
HCC-2998	HL-60(TB)	SF-295	MDA-MB-231
HCT-116	K-562	SF-539	HS578T
HCT-15	MOLT-4	SNB-19	BT-549
HT29	RPMI-8226	SNB-75	T-47D
KM12	SR	U251	MDA-MB-468
SW-620			
Prostate			
PC-3			
DU-145			

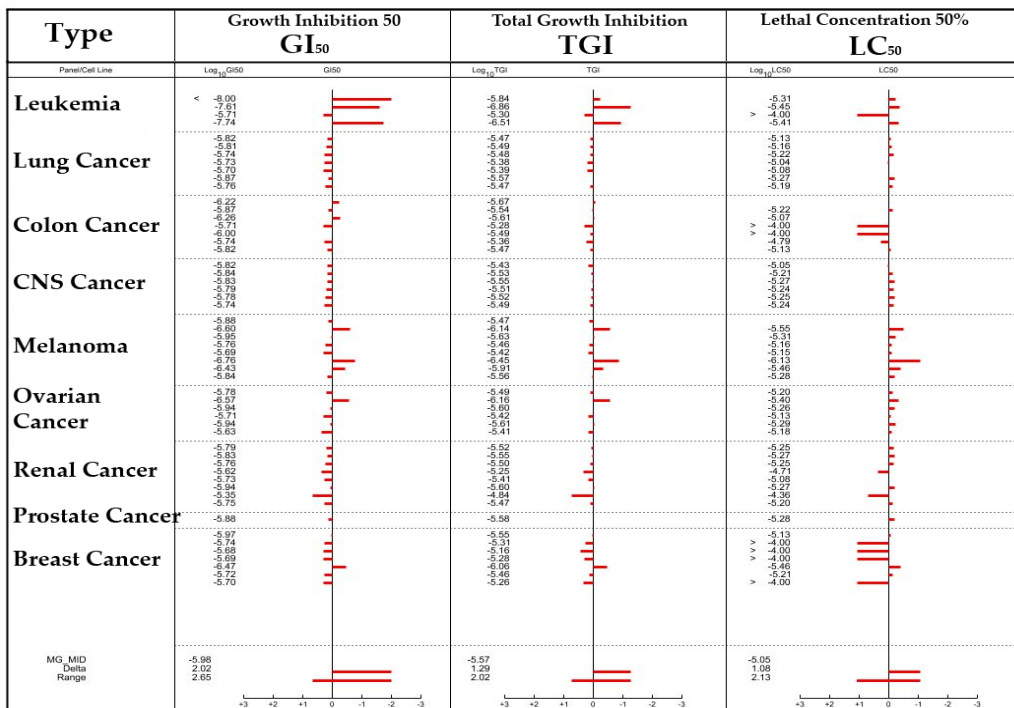
Compounds are screened at five concentrations to determine the GI_{50} , the concentration required to inhibit half of the cell growth, the TGI, the concentration of drug needed for total growth inhibition, and the LC_{50} , the concentration needed to kill half the of tumor cells. These values are extrapolated from the dose response curve produced during the experiment (figure 17). These values provide a measure of potency for the drug, the x-axis gives the \log_{10} of the drug concentration while the y axis gives the optical density of the test culture.

Figure 17. Dose Response Curve



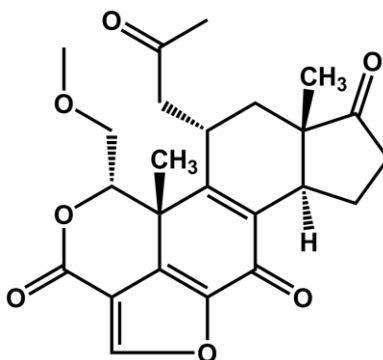
The dose response data is then averaged and reported in a mean graph to show the specificity of the drug for the different types of cancer (Boyd & Paull, 1995) (figure 18). The center line represents the mean concentration for each parameter and the bars to the left or right show how each cell line varies from the mean, the range in the mean graph is a measure of specificity.

Figure 18. Mean Graph Example



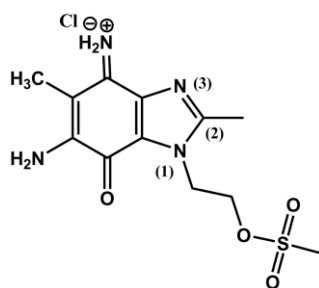
It has been reported that in order for a kinase inhibitor to show specificity, and thus be a potential lead compound, it must have an LC₅₀ value lower than 10 μM. The commonly prescribed PI3K inhibitor wortmannin (figure 19), for example, is reported to have a LC₅₀ value in the low nM range (Baguley & Kerr, 2002) (Knight & Shokat, 2005).

Figure 19: Wortmannin



Dr. Daniel LeBarbera and Dr. Hung Hoang greatly simplified the core active structure through several manipulations; the resulting pharmacophore exchanged the indole core with a benzimidazole core, removed the ethylene tether between the 3 position on the ring and the conjugated amine responsible for the dyes color, and added an alkylating sulfonyl group to a side chain at the two position of the benzimidazole (figure 20).

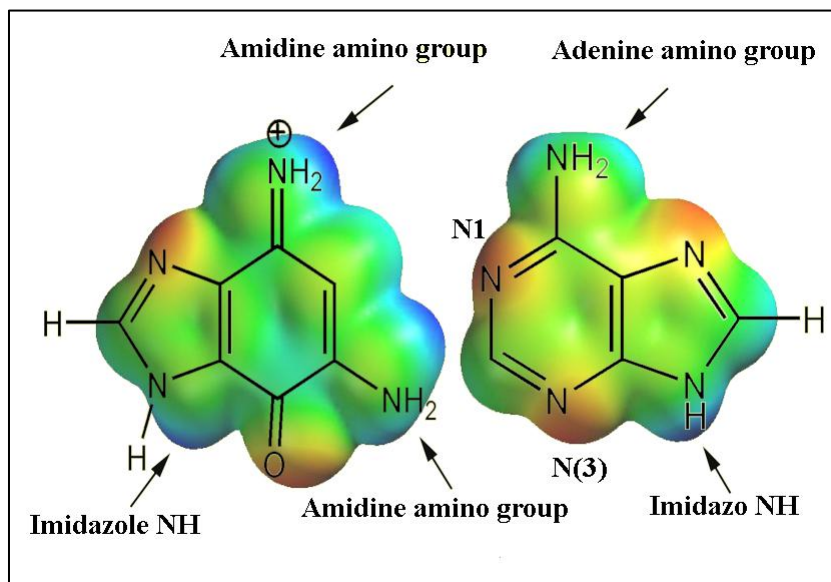
Figure 20: Extended Amidine Pharmacophore



This compound, when screened at the NCI, showed specificity towards lung, melanoma, and colon cancer with activity in the micro molar range. The Developmental Therapeutics Program (DTP) COMPARE program at the NCI was then used to predict possible molecular targets for this new class of compounds. The COMPARE algorithm correlates the histological specificity of the submitted compound against the relative mRNA levels of suspect oncogenic enzymes and proteins (Boyd & Paull, 1995). The new extended amidines were not found to act as topoisomerase poisons like their natural product predecessors, but rather were found to correlate well with cancers containing high levels of BAD, and since the signaling pathways associated with BAD were highly complex network of kinases, Dr. LeBarbera investigated the potential uses of these drugs as ATP anti metabolites. He showed through the use of electrostatic potential maps, that the

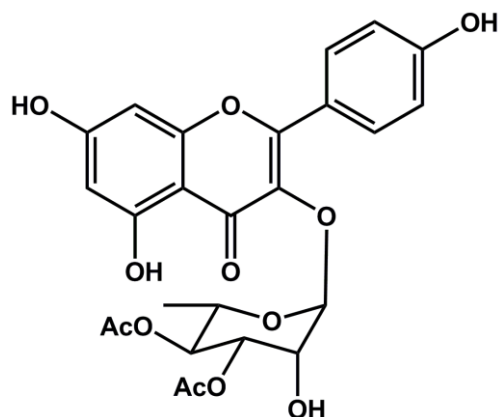
benzimidazole iminoquinone could act as an adenosine mimic (figure 21), the ethylene chain could mimic the sugar, and the sulfonyl group could act as a phosphate mimic, implicating the potential role of these compounds to interact with signal transduction pathways.

Figure 21: Electrostatic Potential Map of the Extended Amidine Core and Adenine



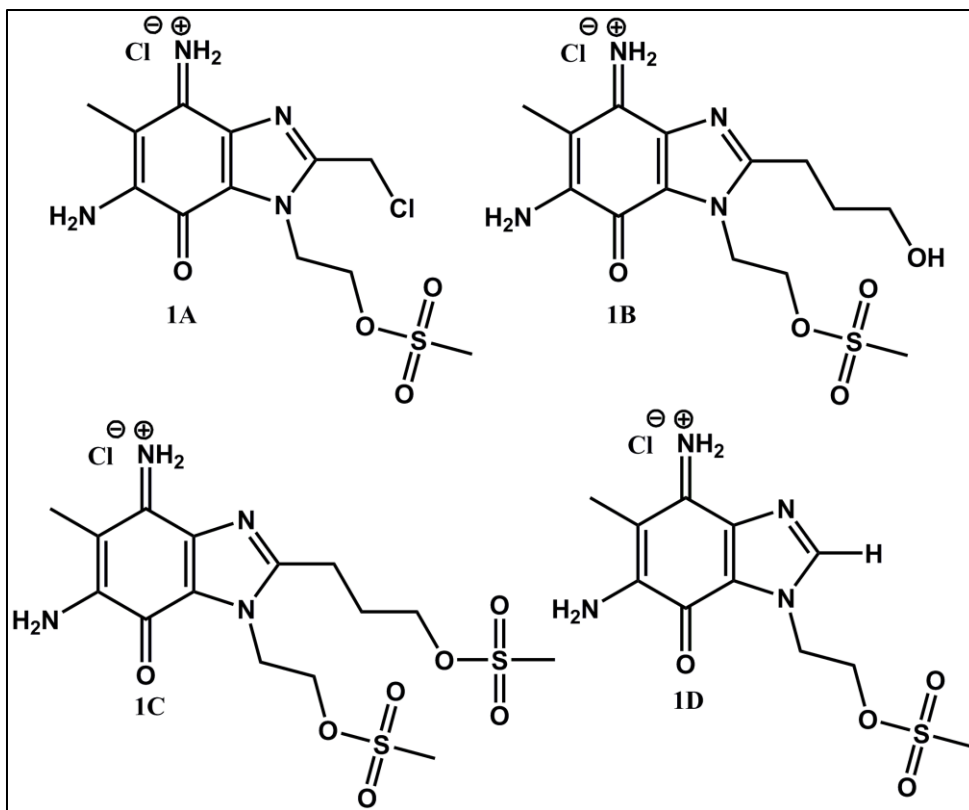
The active sites in kinases, such as those found in the apoptosis signaling pathways, are highly conserved throughout nature making target specificity difficult (Knight & Shokat, 2005) (Hanks, Quinn, & Hunter, 1988). In 2005 a study of p90RSK showed that downstream modification of non conserved cysteine could selectively inhibit the enzymes catalytic activity (Cohen, Zhang, Shokat, & Taunton, 2005). The natural product SL0101 (figure 22) has been shown to specifically target p90RSK, a kinase involved in BAD mediated cell death, with activity in the sub micro molar range (Nguyen et al., 2006).

Figure 22: SL0101



The goal of this research was to synthesize a new class of iminoquinones to specifically target kinases in the PI3K/AKT pathway. These compounds were varied at the 2 position of the imidazole in order to probe residues downstream from the active site using, hydrophobic, alkylating, and hydrogen bonding groups. The synthetic targets (figure 23) were then evaluated for cytotoxicity, and histological specificity using the NCI 60 cell line assay.

Figure 23. Synthetic Targets



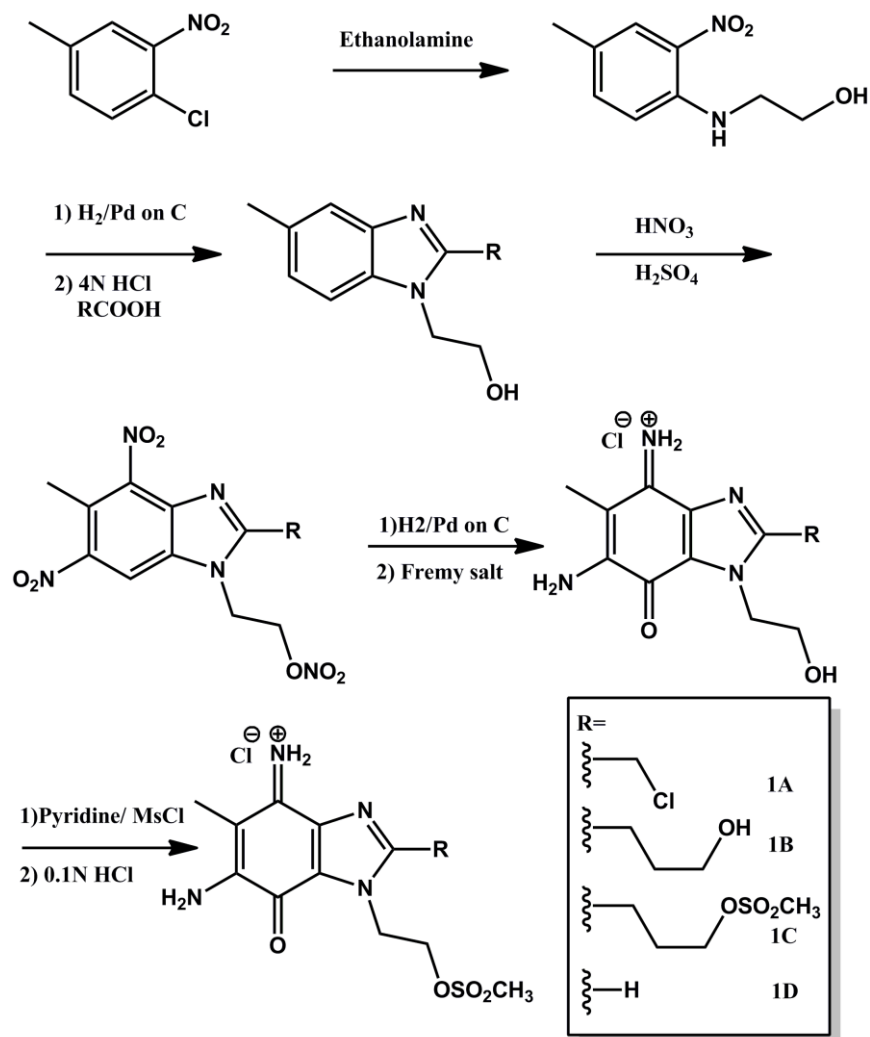
Chapter 2

SYNTHESIS

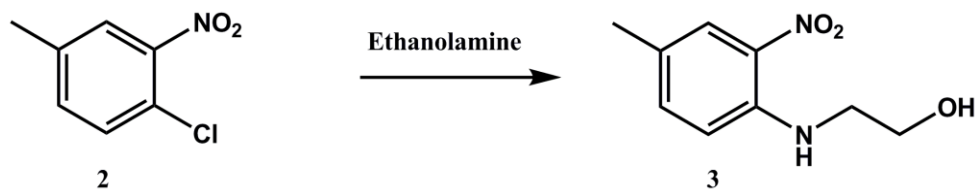
2.1 General Synthesis of 6-Amino-4-imino-1-(2-methansulfonyethyl)-5-methyl-1*H*-benzimidazole-7-ones.

The extended amidine analogs, with substitution at the 2 position, were synthesized in five steps from 4-chloro-3-nitrotoluene, compound 2, following the general synthesis shown in Scheme 1. All extended amidine analog synthesis started with the nucleophilic aromatic substitution of compound 2 using ethanolamine to give compound 3 in 85% yield (Scheme 2).

Scheme 1: General Synthesis of Extended Amidines



Scheme 2. Synthesis of 4-(2-hydroxyethylamino)-3-nitrotoluene (3).

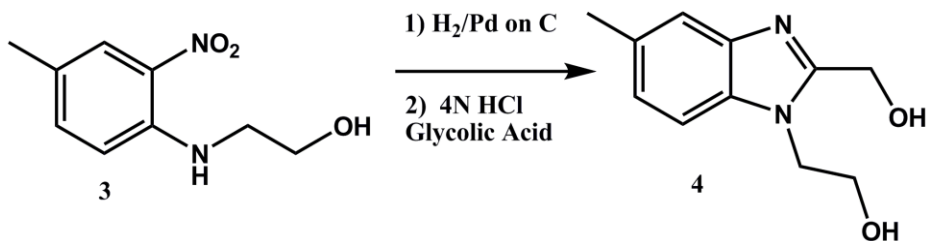


2.2 Synthesis of 6-amino-2-chloromethyl-4-imino-1-(2-methanesulfonyethyl)-5-methyl-1*H*-benzimidazole-7-one (1A).

The preparation of compound 1A, started with the catalytic reduction of compound 3, with 5% palladium on activated carbon, via hydrogenation, followed

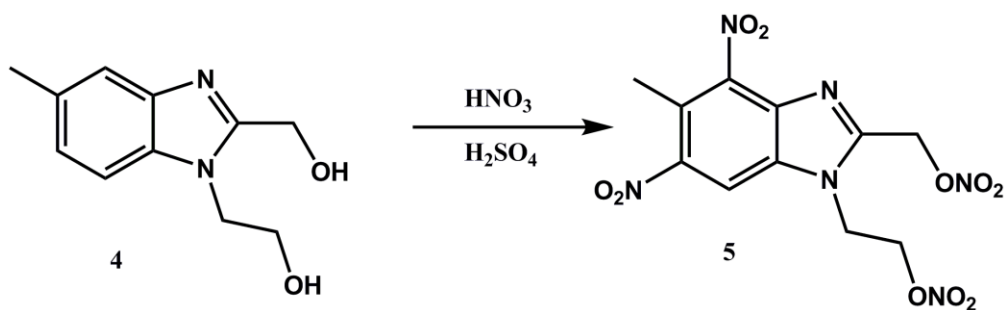
by a Philips reaction, with glycolic acid in 4N HCl, to afford the benzimidazole 4 product in 86% yield (scheme 3).

Scheme 3. Synthesis of 5-methyl-1-(2-hydroxyethyl)-2-hydroxymethyl-benzimidazole (4).



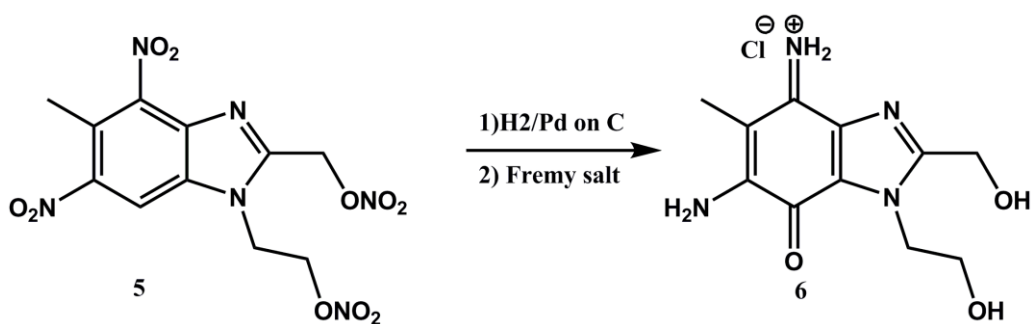
Di-nitration of 4 with concentrated sulfuric and 90% fuming nitric acid gave the electrophilic aromatic substitution product 5 in 60% yield after silica gel column chromatography (scheme 4).

Scheme 4. Synthesis of 4,6-dinitro-5-methyl-1-(2-nitrooxyethyl)-2-nitrooxymethyl-1*H*-benzimidazole (5).

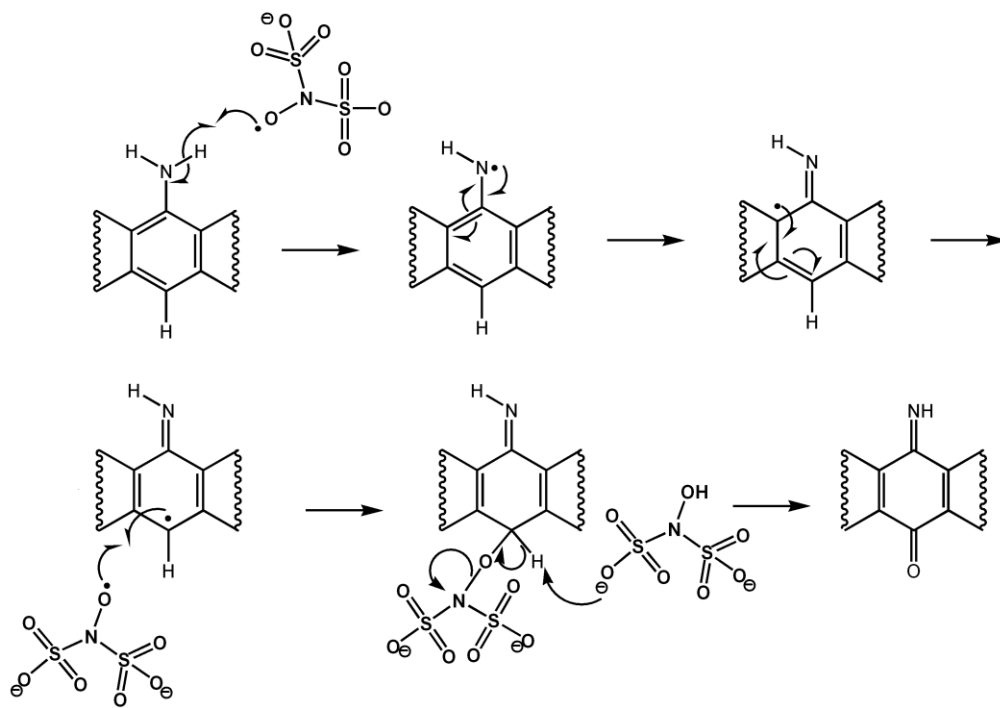


The di-nitration product was catalytically reduced, with palladium on activated carbon, followed by Fremy oxidation to give the purple crystalline hydrochloride salt 6 in 22% yield after C18 reverse phase chromatography (scheme 5).

Scheme 5. Synthesis of 6-amino-4-imino-1-(2-hydroxyethyl)-2-hydroxymethyl-5-methyl-1*H*-benzimidazole-7-one (6).

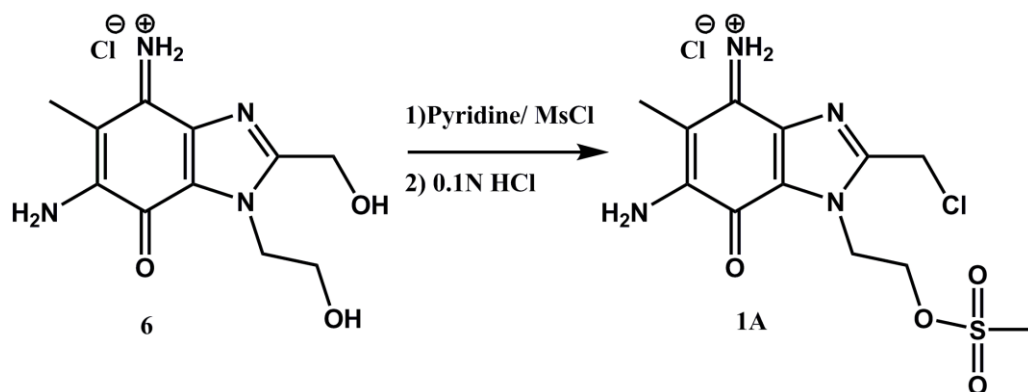


Scheme 6. Mechanism of Fremy Oxidation



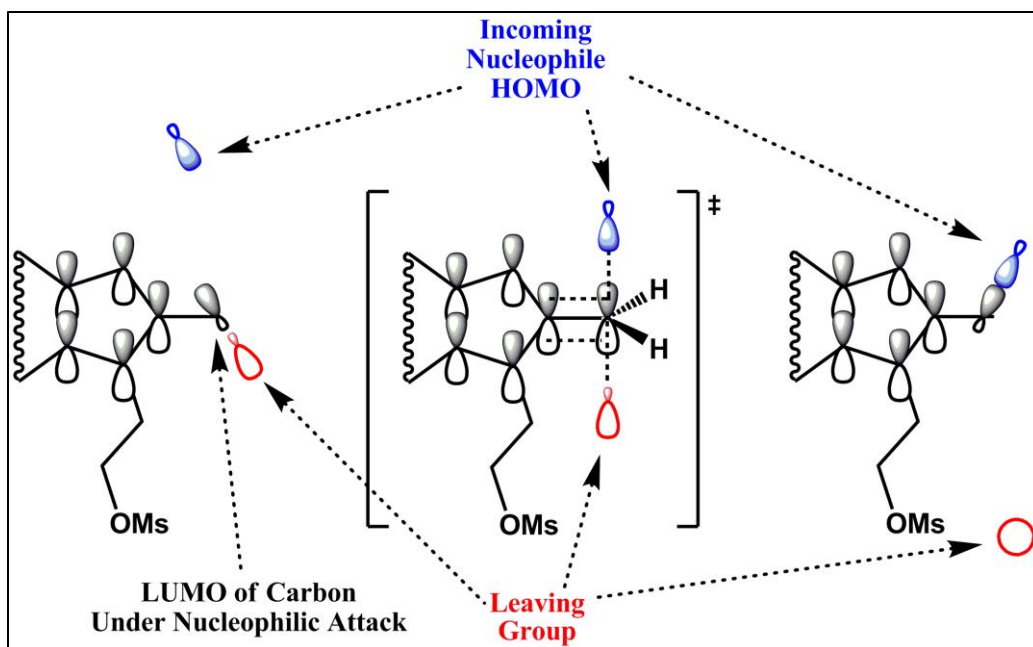
The hydrochloride salt was then sulfonated using methanesulfonyl chloride and pyridine to give substitution product 1A in 23% yield after C18 reverse phase column chromatography and treatment with 0.1M HCl (scheme 7).

Scheme 7. Synthesis of 6-amino-2-chloromethyl-4-imino-1-(2-methansulfonyloxyethyl)-5-methyl-1*H*-benzimidazole-7-one (1A).



The regioselectivity of the chloride and sulfonyl groups can be explained by pi stabilization at the benzyl position (scheme 8). In the presence of dilute hydrochloric acid, the HOMO of the chloride anion, although heavily solvated, is able to attack the LUMO of the carbon bearing the mesylate leaving group in an S_N2 type reaction. The S_N2 transition state becomes planar and aligns the molecular orbital under attack with the conjugated pi system, this provides the stabilization necessary to complete the reaction. Without the pi stabilization at the alkyl mesyl group, this reaction is not able to proceed (Anslyn & Dougherty, 2006).

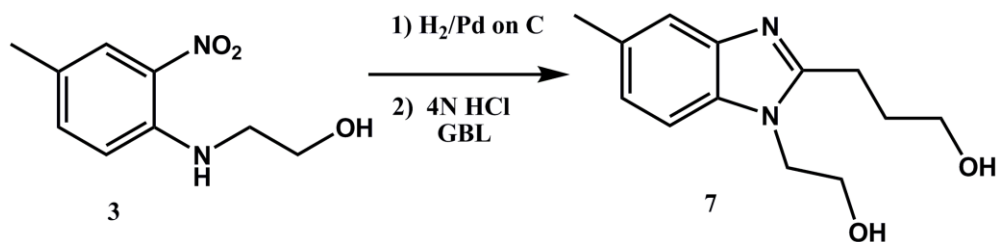
Scheme 8. Regioselective Substitution



2.3 Synthesis of 6-amino-2-hydroxypropyl-4-imino-1-(2-methansulfonyethyl)-5-methyl-1*H*-benzimidazole-7-one (1B) and 6-amino-4-imino-1-(2-methansulfonyethyl)-2-methansulfonypropyl-5-methyl-1*H*-benzimidazole-7-one (1C).

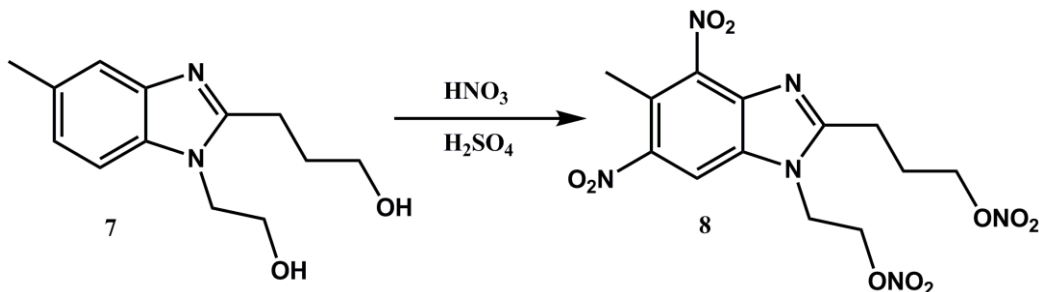
The synthesis of 1B and 1C began with the catalytic reduction of compound 3, with 5% palladium on activated carbon, via hydrogenation, followed by a Philips reaction, with *gamma*-butyrolactone in 4N HCl to afford the benzimidazole product 7 in 84% yield (scheme 9).

Scheme 9. Synthesis of 5-methyl-1-(2-oxyethyl)-2-oxypropyl-benzimidazole (7)



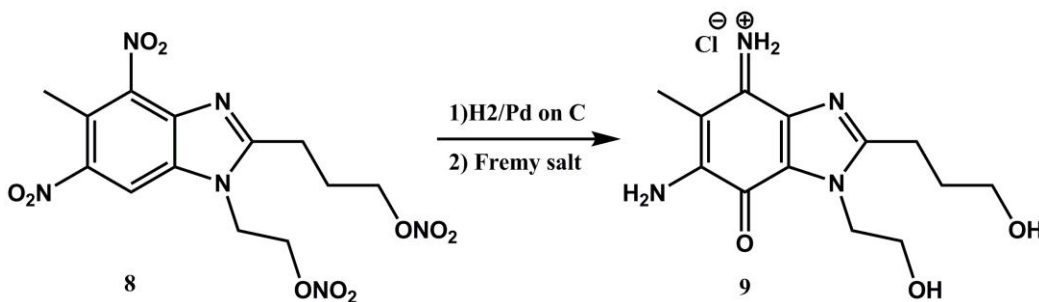
Di-nitration of 7 with concentrated sulfuric and 90% fuming nitric acid gave the electrophilic aromatic substitution product 8 in 59% yield after silica gel column chromatography (scheme 10).

Scheme 10. Synthesis of 4,6-dinitro-5-methyl-1-(2-nitrooxyethyl)-2-nitrooxypropyl-1*H*-benzimidazole (8).



The di-nitration product was catalytically reduced, with palladium on activated carbon, followed by Fremy oxidation to give the purple crystalline hydrochloride salt 9 in 87% yield after C18 reverse phase chromatography (scheme 11).

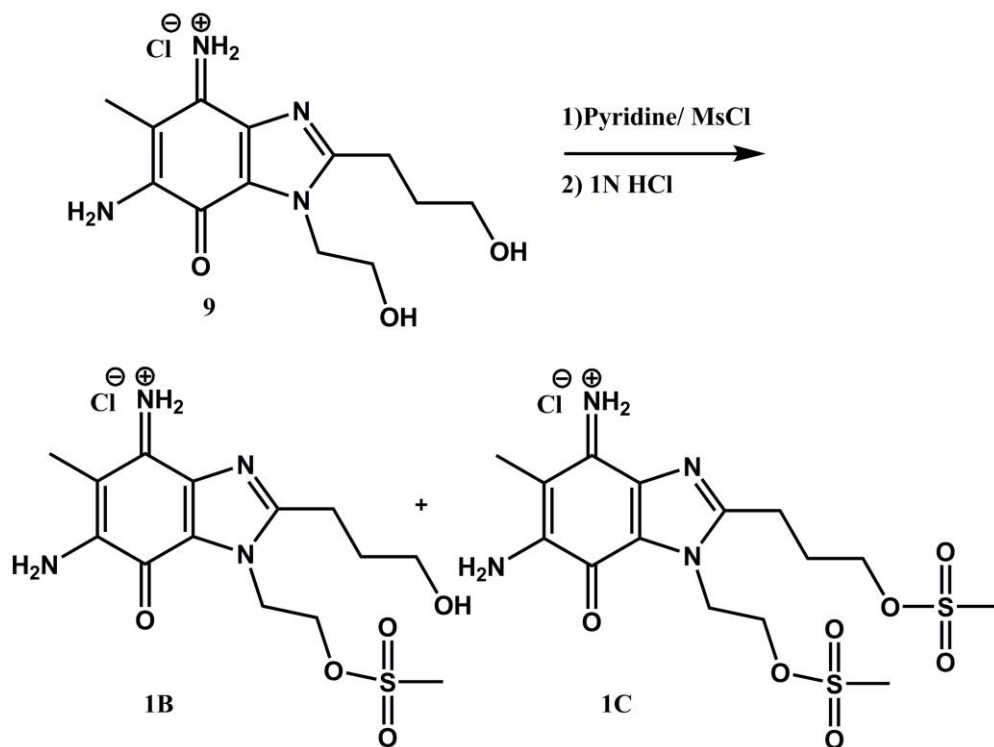
Scheme 11. Synthesis of 6-amino-4-imino-1-(2-hydroxyethyl)-2-hydroxypropyl-5-methyl-1*H*-benzimidazole-7-one (9).



The hydrochloride salt was then sulfonated using methanesulfonyl chloride and pyridine to give substitution product 1B in 17% yield and product 1C

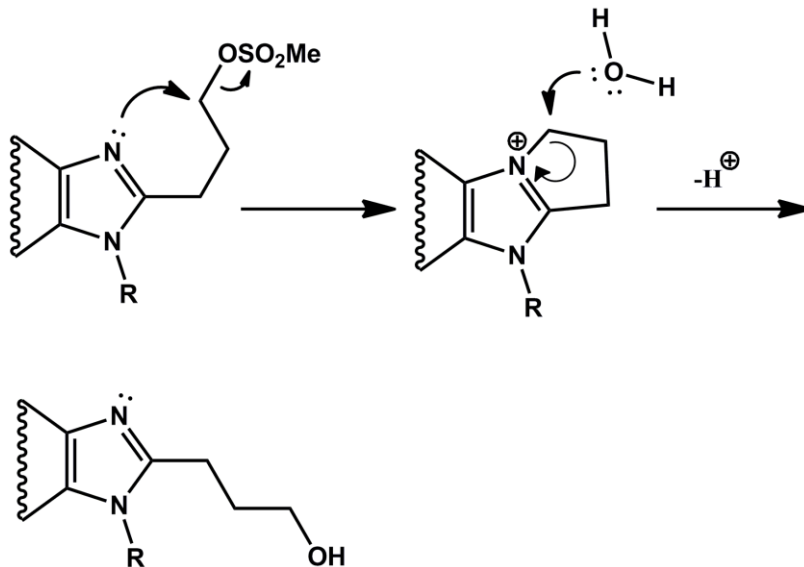
in 20% yield after C18 reverse phase column chromatography and treatment with 1M HCl (scheme 12).

Scheme 12. Synthesis of 6-amino-2-hydroxypropyl-4-imino-1-(2-methansulfonyxyethyl)-5-methyl-1*H*-benzimidazole-7-one (1B) and 6-amino-4-imino-1-(2-methansulfonyxyethyl)-2-methansulfonyxypropyl-5-methyl-1*H*-benzimidazole-7-one (1C).



The reason for the observed regioselectivity can be explained by anchimeric assistance. The orthogonal lone pair on the nitrogen at the 3 position of the imidazole can attack the mesylate bearing carbon in an S_N2 type reaction to form a strained 5 membered iminium intermediate. The electrophilic carbon attached to the iminium center can then be attacked by water followed by deprotonation to give the regioselective product (Anslyn & Dougherty, 2006) 1B (scheme 13).

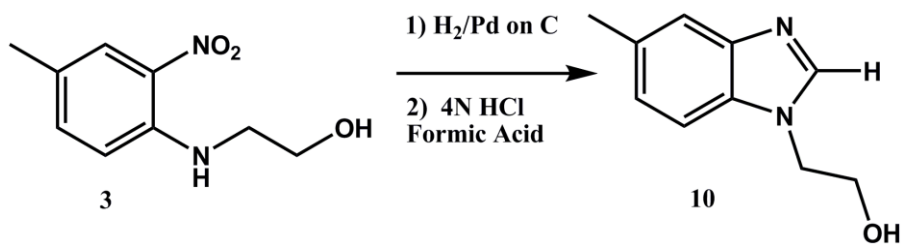
Scheme 13. Regioselectivity of Sulfonation Due to Anchimeric Assistance.



2.4 Synthesis of 6-amino-4-imino-1-(2-methansulfonyxyethyl)-5-methyl-1*H*-benzimidazole-7-one (1D).

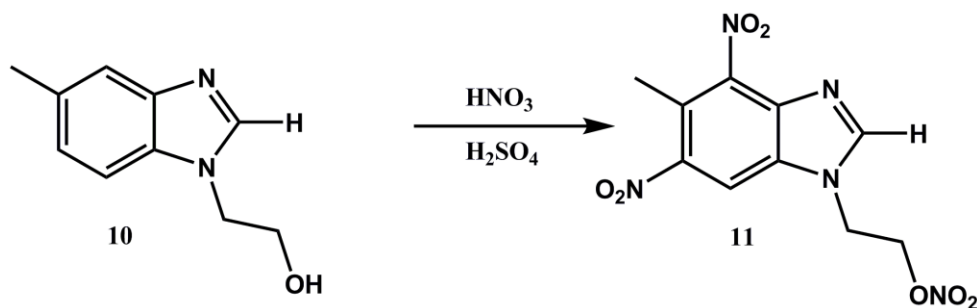
The preparation of compound 1D, started with the catalytic reduction of compound 10, with 5% palladium on activated carbon, via hydrogenation, followed by a Philips reaction, with formic acid in 4N HCl, to afford the benzimidazole 10 product in 81% yield (scheme 14).

Scheme 14. Synthesis of 1-(2-Hydroxyethyl)-5-methylbenzimidazole (10).



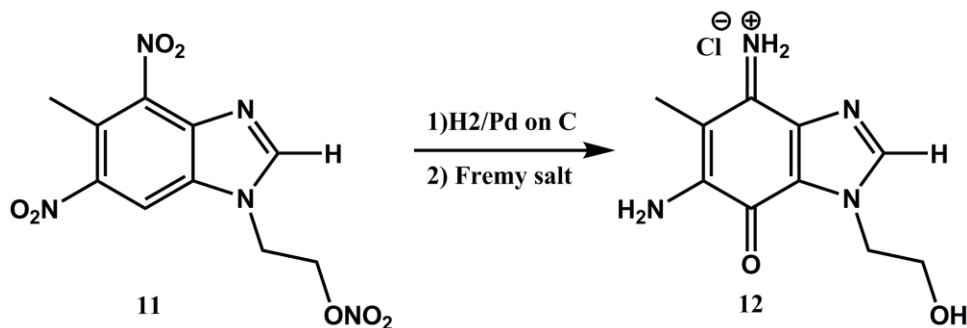
Di-nitration of 10 with concentrated sulfuric and 90% fuming nitric acid gave the electrophilic aromatic substitution product 11 in 86% yield after silica gel column chromatography (scheme 15).

Scheme 15. Synthesis of 4,6-dinitro-5-methyl-1-(2-nitrooxyethyl)-*1H*-benzimidazole (11).



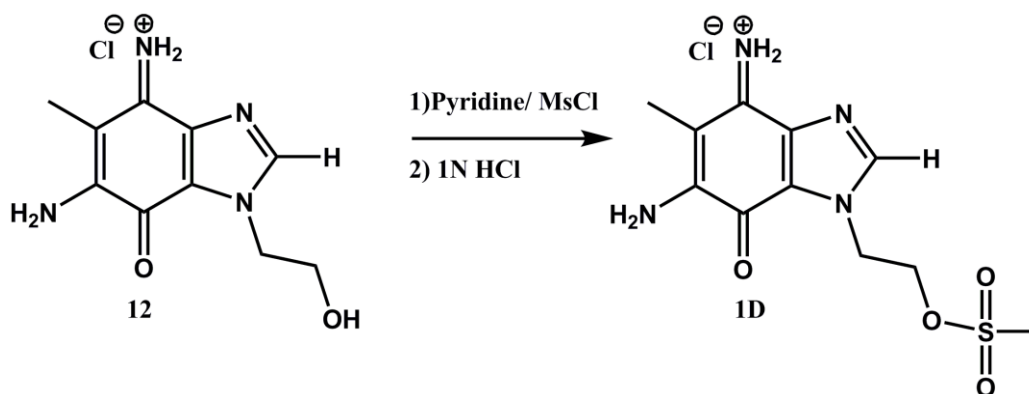
The di-nitration product was catalytically reduced, with palladium on activated carbon, followed by Fremy oxidation to give the purple crystalline hydrochloride salt 12 in 80% yield after C18 reverse phase chromatography (scheme 16). This product was immediately sulfonated without characterization.

Scheme 16. Synthesis of 6-amino-4-imino-1-(2-hydroxyethyl)-5-methyl-*1H*-benzimidazole-7-one (12).



The hydrochloride salt was then sulfonated using methanesulfonyl chloride and pyridine to give substitution product 1D in 52% yield after C18 reverse phase column chromatography and treatment with 1N HCl (scheme 17).

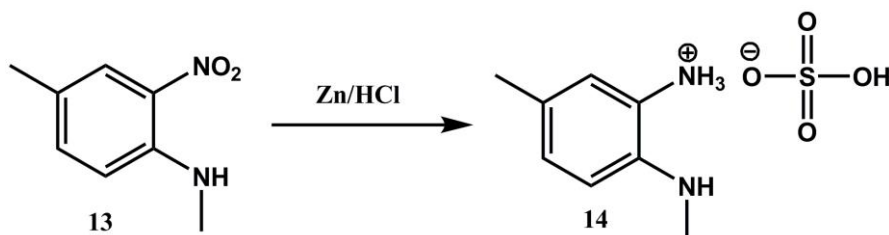
Scheme 17. Synthesis of 6-amino-4-imino-1-(2-methanesulfonyloxyethyl)-5-methyl-*1H*-benzimidazole-7-one (1A).



2.5 Synthesis of 1,5-dimethyl-1*H*-benzimidazole-2-methanamine (15).

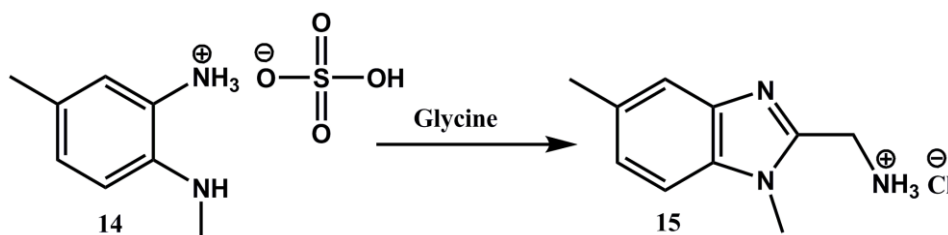
The synthesis of compound 15 began with commercially available, N,4-dimethyl-2-nitroaniline, compound 13, which was catalytically reduced, with Zn metal and HCl, and isolated as the bisulfate salt 14 in 77% yield (scheme 18).

Scheme 18. Synthesis of N,3-dimethyl-2-aminoaniline (14).



Compound 14 was then treated with glycine to give compound 15 in 83% yield as a hydrochloride salt (scheme 19)

Scheme 19. Synthesis of 1,5-dimethyl-1*H*-benzimidazole-2-methanamine (15).



Chapter 3

RESULTS AND DISCUSSION

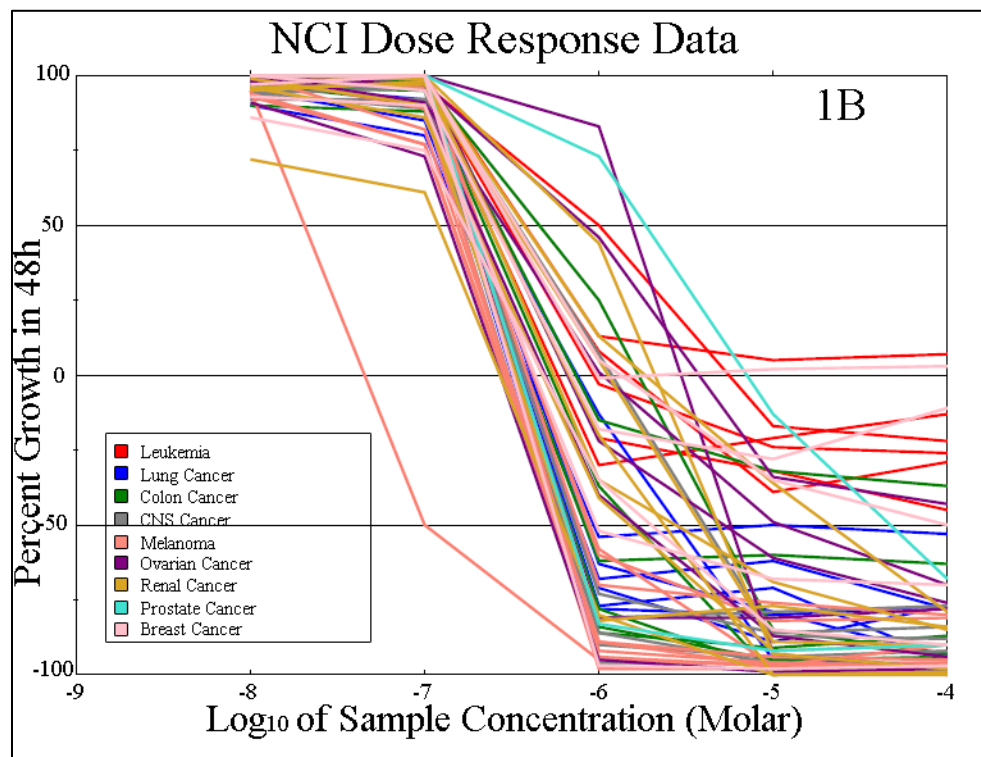
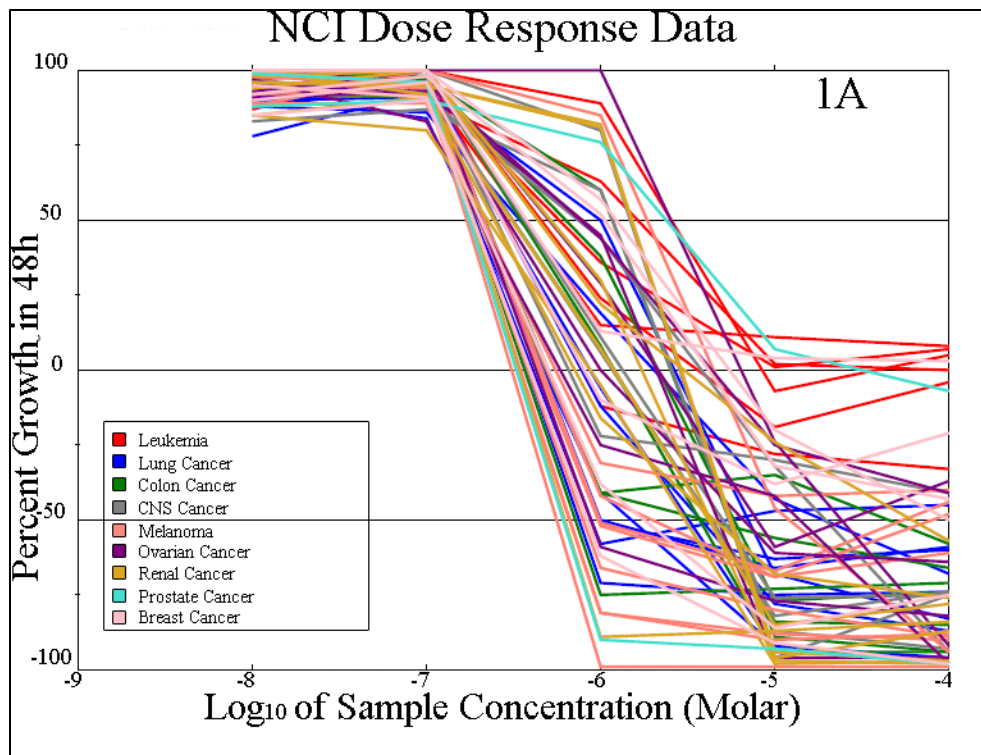
3.1 NCI Cell Line Studies

Each target compound was submitted to the NCI DTP to be assayed against 60 different human tumor cell lines to gauge the potency of each drug as well as the selectivity for each cancer type. Only compounds 1A and 1B have completed cell line data, data on compound 1C and 1D will be reported at a later date. The relevant data extracted from each NCI DTP cell line report is the dose response data and the mean graph data. The dose response data, which tells you the GI_{50} , TGI, and LC_{50} , was used to gauge the potency of the submitted compound, while the mean graph was used to gauge the specificity of the submitted compounds (Boyd & Paull, 1995).

3.2 Potency of Compounds 1A and 1B

The GI_{50} , TGI, and LC_{50} are all reported in the dose response curves for each compound (figure 24), only the LC_{50} will be discussed for each compound since this new class of iminoquinones were designed as apoptosis inducing drugs.

Figure 24. Dose Response Data for Compound 1A and 1B



Both compound 1A and 1B had an average LC_{50} in the sub μM range, while the lowest values for 1A and 1B were 561nM and 102nM respectively. This puts the potency of each drug in the acceptable sub μM range and just on the cusp of the most prescribed and useful chemotherapeutic agents which typically fall in the low nM range. Potency alone is not enough to determine a potential lead compound, for example, a compound with a low nM activity that shows no specificity in the mean graph is likely cytotoxic to all cells. Establishing specificity so that certain cancer lines show low activity at high concentration and high activity at low concentration suggests the drug is working on a specific target, rather than being toxic to any biological cell.

3.3 Specificity of Compounds 1A and 1B

The mean graphs are created by first finding the average value of a specific set of dose response data, for example, in order to obtain a mean graph the average LC_{50} must first be calculated. This value is then used as the midline so that the bars to the left of the midline represent compounds with lower potency than average, and compounds to the right of the midline represent compounds with higher potency than the average. The \log_{10} values are used so that one unit represents an order of magnitude change in potency (Boyd & Paull, 1995). The mean graphs for both 1A and 1B are shown in figure 25 and figure 26 respectively.

Figure 25. Mean Graph of Compound 1A

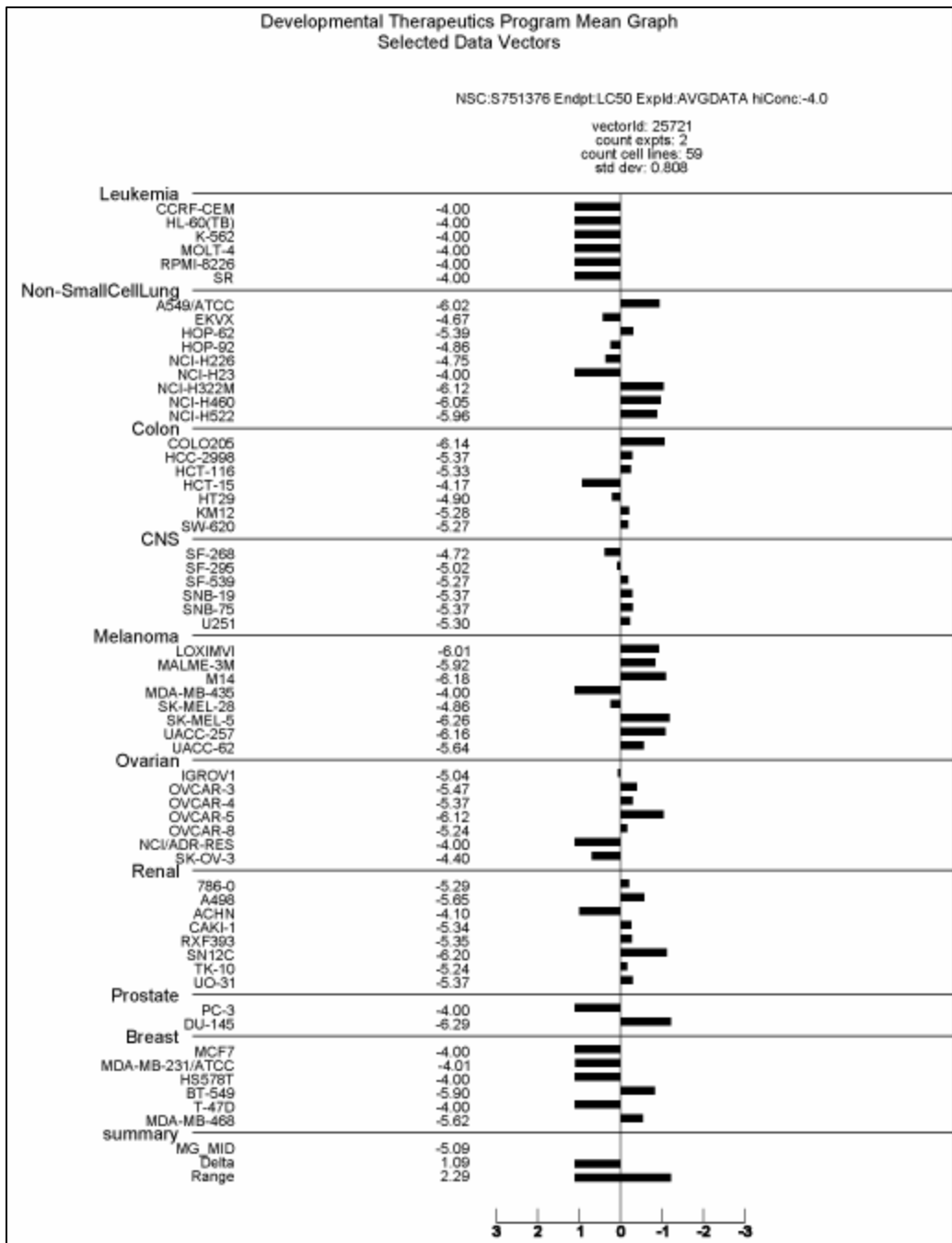
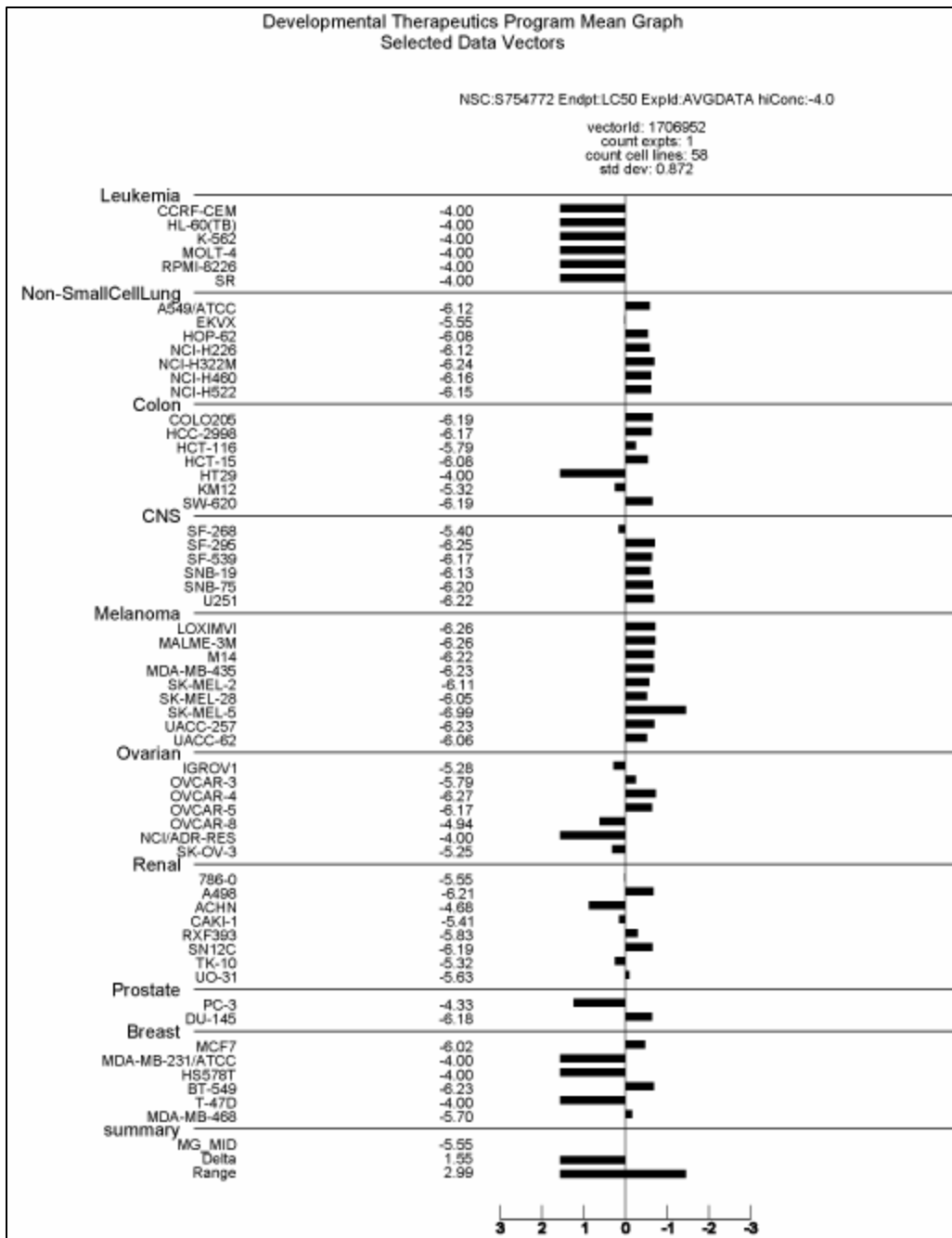


Figure 26. Mean Graph of Compound 1B



The range of values for 1A and 1B is 2.3 and 3.0 respectively, this means that 1B, for example, is 1000-fold more specific for the SK-MEL-5 melanoma cell line than any leukemia cell lines. The regional topology for a specific cancer type, melanoma for example, shows specificity compared to regions of little to no

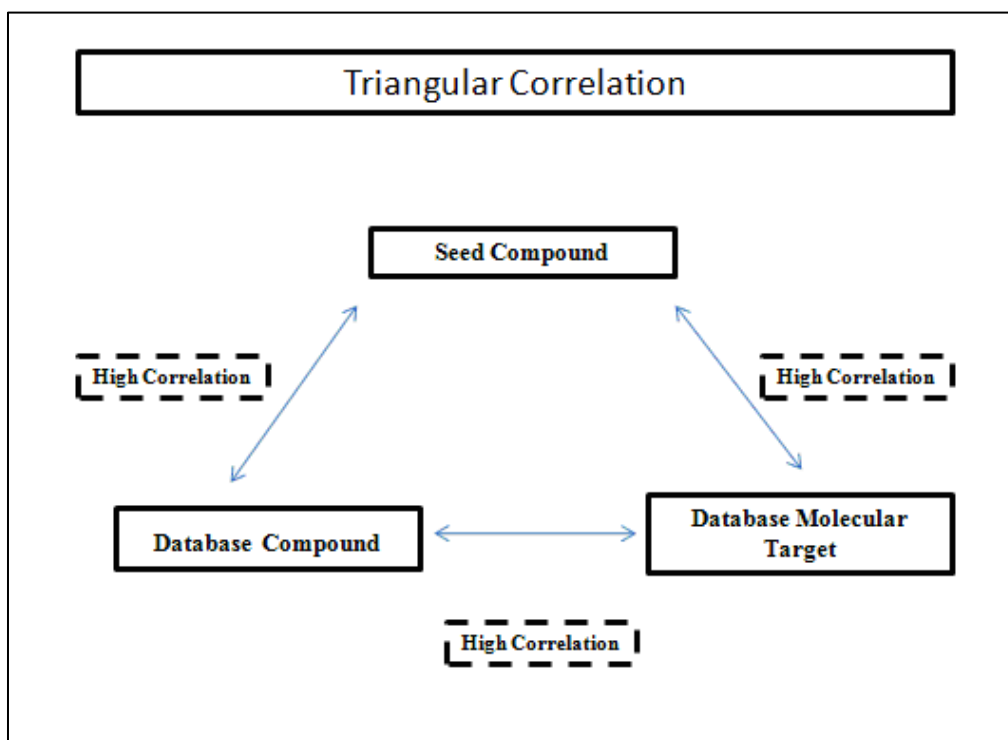
specificity, as in the case of leukemia for both compound 1A and 1B. Compound 1A showed specificity towards lung cancer and melanoma cell lines, while compound 1B showed specificity for lung, colon, CNS, and melanoma cell lines with an average 100 fold greater activity when compared to leukemia. With an acceptable potency and specificity established, the DTP COMPARE algorithm was used to shed insight on the mechanism of action and potential molecular targets.

3.4 DTP COMPARE

The mean graph topology can be thought of as a fingerprint of biological activity for each compound, theoretically the mean graph should look the same each time the cell line experiments are run. The topology of compounds 1A and 1B were compared to the DTP database which contains two important sets of data. First, the DTP has data on nearly 100,000 compounds that have been previously submitted and screened through the NCI DTP. This data contains not only the dose response and mean graph data, but also accounts for any known molecular targets and mechanism of action reported for each compound. The second subset of the database comprises mean graph data of molecular target levels in each cell line, this data is typically measured using DNA microarray experiments of the target in question. This gives the ability to correlate the mean graph of the seed compound to the mean graph of any molecular target in the database (Boyd & Paull, 1995). These tools allow for an additional depth of analysis using triangular correlation where a seed compound correlates with both a compound from the database and a molecular target from the database (figure

27). If the database compound and molecular target are found to correlate well, then the triangular correlation is confirmed along with the proposed mechanism and target of the seed compound. The inability to correlate above well with a database compound and/or a molecular target suggests a potential new mechanism that has not been elucidated or reported by the NCI DTP.

Figure 27. Triangular Correlation



The initial compare using synthetic and natural product databases failed to correlate compound 1A and 1B to any structure with a known target, this made it difficult to form any triangular correlation. Instead, a COMPARE matrix was set up to correlate compounds 1A and 1B and the two most promising extended amidine compounds synthesized by Dr. Daniel LeBarbera in this lab, compounds 736296 and 732650 (Figure 28), this data is shown in table 2.

Figure 28. Compounds 736296 and 732650

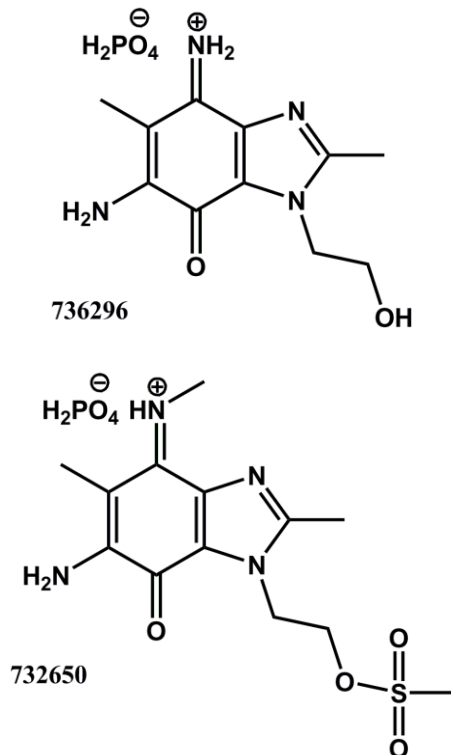


Table 2. Matrix Compare Correlation Coefficients of 1A, 1B, 736296 and 732650

COMPARE Matrix for 1A, 1B, 736296, 732650				
Seed	1B	1A	736296	732650
1B	1			
1A	0.77	1		
736296	0.53	0.36	1	
732650	0.52	0.3	0.42	1

This matrix shows that the new compound 1A and 1B correlate well with each other at 77%, which is 24% higher than the next closest compound, 736296. This suggests that compound 1A and 1B share similar mechanisms of action distinct from the class of compounds they were based on. Once this was established, each compound was compared to the molecular target microarray database.

Interestingly compound 1A and 1B correlated best with sequestosome 1

(SQSTM1) at 57.4% and 68.2% respectively. A matrix COMPARE was set up using compound 1A and 1B, and included molecular target mean graph data for SQSTM1 as well as the two Bcl-2 death proteins BAD and BAX (Table 3).

Table 3. Molecular Target Compare Correlation Coefficients Matrix

Matrix Compare of 1A and 1B Against Molecular Targets BAX, BAD, and SQSTM1					
Seed	1A	1B	BAX	BAD	SQSTM1
1A	1				
1B	0.77	1			
BAX	-0.11	0.05	1		
BAD	0.39	0.5	0.14	1	
SQSTM1	0.57	0.68	0.06	0.49	1

This shows that the new class of compounds submitted do correlate best with SQSM1, but also slightly correlate to BAD, furthermore SQSM1 seems to correlate with BAD to about the same degree as the compounds do. The mean graph data for 1A and 1B were superimposed on the mean graph of SQSM1 to visually represent this correlation coefficient by cell line (figure 29).

Figure 29. Mean Graph Data of 1A Over SQSM1 and 1B Over SQSTM1 by Cancer Panel

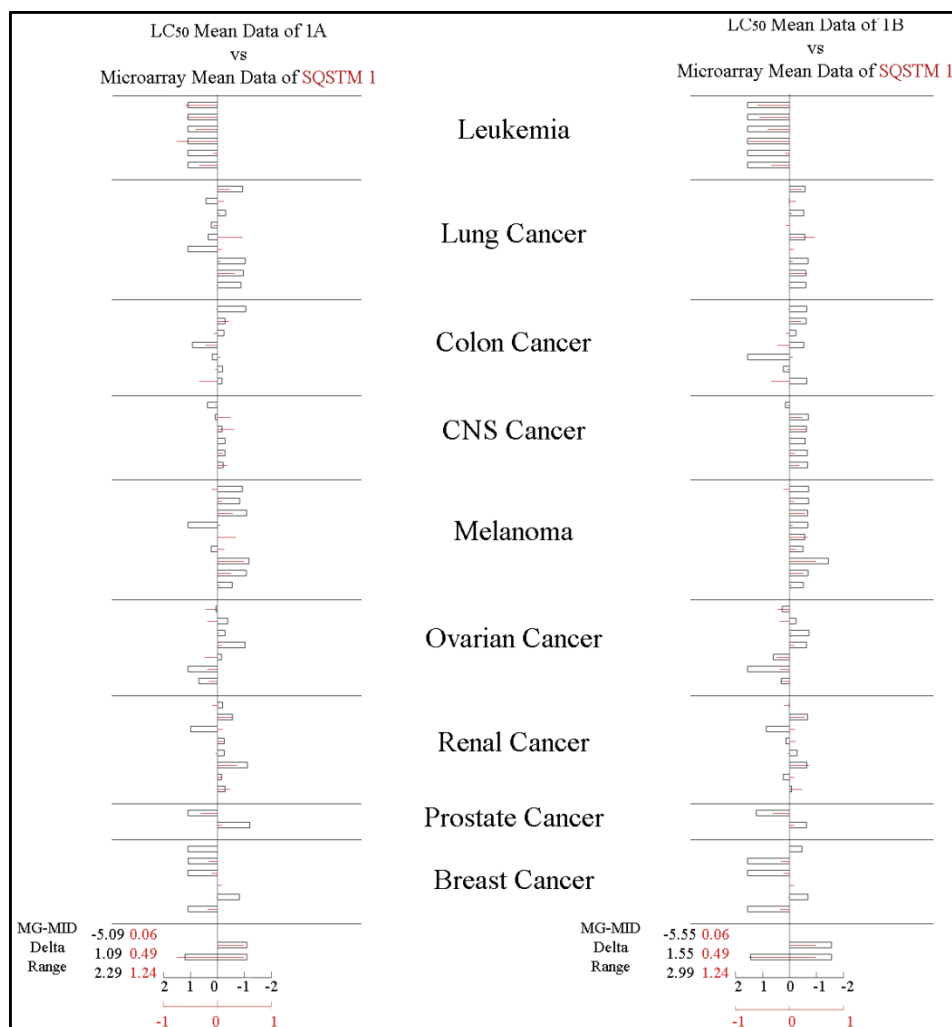
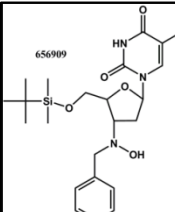


Figure 29 shows that the general trend of target expression of SQSTM1 and compound specificity for 1A and 1B follow similar trends. Although SQSTM1 was not the intended target, it does play a role in various cancers. The majority of research on the role of SQSTM1 in cancer was published within the last five years and its mechanism has not fully been elucidated yet. It seems to be a key player in cancer cell survival through regulation of autophagy and also plays a role in drug resistance in certain cancer types (Puissant et al., 2010). SQSTM1 has also been shown to be intimately linked to Necrosis Factor Kappa Beta (NF- κ B) (Puissant et al., 2010). This kinase is involved in an alternative apoptosis pathway that begins

with the phosphorylation of protein kinase C (PKC) by PI3K, a kinase implicated in the originally proposed mechanism for the compounds synthesized by Dr. LaBarbera. An interesting study using SQSTM1 knock out experiments was able to reduce drug resistance in resilient leukemia cells (Puissant et al., 2010), this proposes an interesting hypothesis for compounds 1A and 1B. If they do specifically target SQSTM1 and if SQSTM1 is responsible for drug resistance, then a synergistic effect should be observed when co administered with a potent clinical drug.

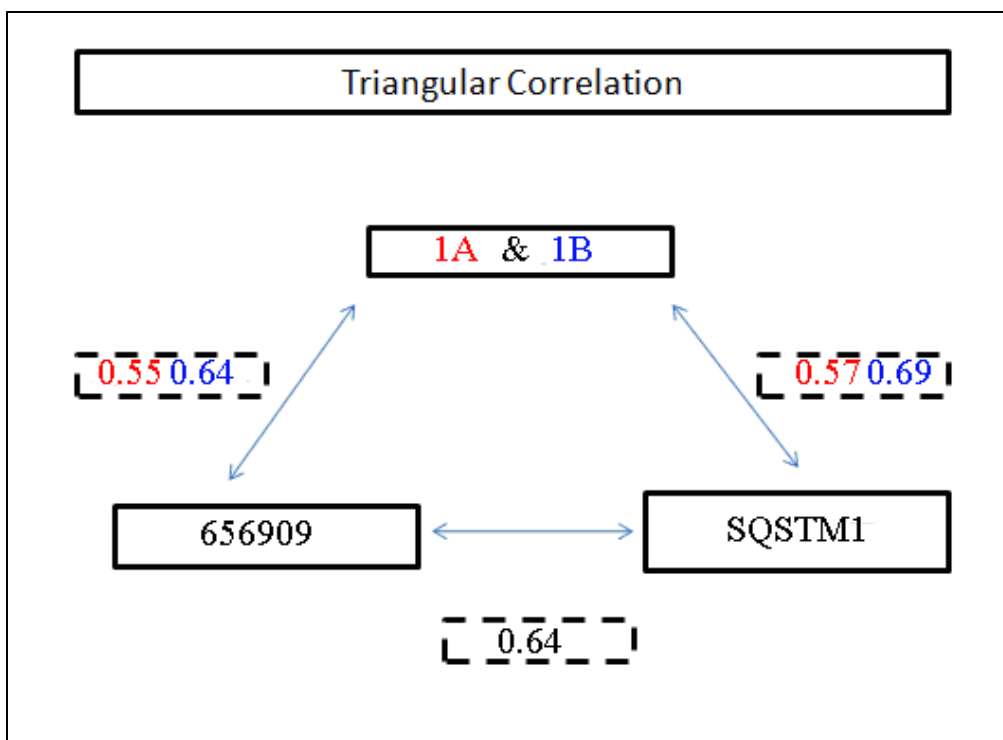
Finally, the mean graph data for SQSTM1 was used as a seed to back correlate and find other synthetic compounds with similar activity (table 4).

Table 4. Back Correlation of SQSTM1

	Seed	SQSTM1	1B	1A	S656125	S656909
	SQSTM1	1				
	1B	0.69	1			
	1A	0.57	0.74	1		
	S656125	0.5	0.67	0.53	1	
	S656909	0.64	0.64	0.55	0.57	1

This data shows that compound 1A and 1B correlate better with SQSTM1 than any other compound in the DTP database. What is interesting is that out of nearly one hundred thousand entries in the database, the second highest result, 656125, is also an extended amidine iminoquinone suggesting a potential pharmacological role of this moiety in the mechanism. The triangular correlation shown in figure 30 depicts how each component correlates to one another using the DTP database.

Figure 30: Triangular Correlation of 1A/1B, SQSTM1 and 656909



The potency of these back correlated compounds is between 10-100 μ M, this high concentration range makes compound 1A and 1B better candidates for inhibition of an SQSTM1 related cancer pathways.

Chapter 4

CONCLUSION

In conclusion, an efficient strategy for the synthesis of iminoquinones with substitution at the 2 position of the benzimidazole ring has been described and reported. Two interesting mechanisms for diversification have been described during the sulfonation step to give a variety of substitution patterns. Using intermediate stabilization or anchimeric assistance, new analogs can be made without altering previous steps in the synthetic pathway, in the future these regioselective strategies will be used in the synthesis of analogs.

This new class of iminoquinone ATP mimics, with substitution at the 2 position, have shown promising potency and specificity, although they did not correlate well with the intended targets in the AKT pathway. They did however correlate with SQSTM1, a regulatory protein recently found to promote cell survival through autophagy stabilization. The future of this project will focus on expanding the library list through further variation at the 2 position, and must encompass biological assays to verify the molecular target. Once a molecular target is verified, whether it be SQSTM1 or not, the active site can be modeled for a more rational approach to drug design. The potential role of SQSTM1 in cell survival also implicates the need for synergistic studies by co administration with other drugs in cell lines known for high resistance.

Chapter 5

EXPERIMENTAL

5.1 General Experimental

All ¹H-NMR spectra were run at the Magnetic Resonance Research Center at Arizona State University using a 400MHz Varian liquid state spectrometer, all chemical shifts are relative to TMS. IR spectra were taken as KBr pellets and the strongest absorbances reported. All mass spectrometry analyses were run at the High Resolution Mass Spectrometry lab at Arizona State University with the JEOL Cmate spectrophotometer in atmospheric pressure chemical ionization (APCI+) mode. Melting points were recorded using a Mel-Temp® apparatus and are reported uncorrected. All TLCs were performed on plastic-backed silica gel paper using a variety of solvents, visualization was carried out using 254nm UV light. All *in vitro* cell line data was performed through the Developmental Therapeutics Program at the National Cancer Institute (Frederick, MD).

5.2 Synthesis of Listed Compounds

Synthesis of 4-(2-hydroxyethylamino)-3-nitrotoluene (3). Compound 3 synthesized as previously reported (Hoang et al., 2007). 16g (0.093 moles) of 4-chloro-3-nitrotoluene was added to 6g (0.187 moles) of ethanolamine and refluxed for 2 hours. The reaction was then cooled to room temperature and extracted 3x with dichloromethane and dried over sodium sulfate. The dichloromethane was removed under reduced pressure and titrated with hexanes over a 2 hour period to slowly crystallize the produce. The resulting red crystals

were filtered, washed with hexane, and then dried to give 15.5g (85% yield); mp 78-80 °C; TLC (Chloroform/Methanol (90:10)) $R_f=0.44$; IR (KBr pellet) 3445, 3346, 2957, 2926, 2872, 1637, 1568, 1523, 1433, 1406, 1356, 1311, 1219, 1178, 1151, 1039, 922, 812 cm^{-1} ; ^1H NMR (CDCl_3) δ 7.98 (s, 1H, aromatic proton), 7.29 (d, $^3J= 8.7\text{Hz}$, 1H, aromatic proton), 6.83 (dd, $^3J= 8.7\text{Hz}$, 1H, aromatic proton), 3.95 (t, $J = 4.8 \text{ Hz}$, 2H, methylene protons), 3.53 (t, $^3J = 4.8\text{Hz}$, 2H, methylene protons) 2.27 (3H, s, methyl protons); MS (EI mode) m/z 196 (M^+).

Synthesis of 5-methyl-1-(2-oxyethyl)-2-oxymethyl-benzimidazole (4). A suspension of 8g (0.041 moles) of 3 was suspended in 300ml of 4N HCl and reduced under 50 psi of H_2 in the presence of 200mg of 5% Pd on carbon for 24 h. The catalyst was then filtered off using Celite as a filtering aid. 6.2g (0.081 moles) of glycolic acid was added to the filtrate, the resulting solution was then refluxed for one hour. The reaction was first cooled to room temperature, and then placed on an ice bath and made basic (pH=10) using ammonium hydroxide. The white precipitate was filtered off and recrystallized in ethanol to give 6.8g of compound 4 (86% yield); mp 140-141°C; TLC (Chloroform/Methanol (90:10)) $R_f=0.31$; ^1H NMR (CDCl_3) δ 7.39 (d, $^3J= 8.8\text{Hz}$, 1H, aromatic proton), 7.34 (s, 1H, aromatic proton), 7.02 (dd, $^3J= 8.7\text{Hz}$, 1H, aromatic proton), 5.48 (t, $^3J=7.2\text{Hz}$, 1H, alcohol proton), 4.96 (t, $^3J=6.6\text{Hz}$, 1H, alcohol proton), 5.19 (d, $^3J=7.2\text{Hz}$, 2H, methylene protons), 4.34 (t, $^3J= 7.2\text{Hz}$, 2H, methylene protons), 3.70 (q, $^3J= 5.3\text{Hz}$, 2H, methylene protons), 3.32 (s, 3H, methyl protons).

Synthesis of 4,6-dinitro-5-methyl-1-(2-nitrooxyethyl)-2-nitrooxymethyl-1*H*-benzimidazole (5). 1g (0.0048 moles) of 4 was dissolved in a minimal

amount of concentrated sulfuric acid, this solution was then set on an ice bath and cooled to 0°C. 1.2g (0.019 moles) of 90% fuming nitric acid was added to the solution drop wise while paying careful attention to not allow the temperature to rise above 10°C. Once the addition was complete, the solution was stirred at room temperature for 24 h till one spot remained on TLC. This solution was then neutralized with saturated sodium bicarbonate (pH=8) and extracted 3x with ethyl acetate. The organic solvent was then removed under reduced pressure to give a light yellow oil. It was common for new spots on the TLC to form after work up, these compounds were characterized and found to be the hydrolysis products of the nitrate esters. This oil was recrystallized in methanol to give 1.1g of compound 5 (60% yield) as a white crystal; mp 119-120°C; TLC (Ethyl acetate) $R_f=0.78$; IR (KBr Pellet) 3266, 1641, 1593, 1535, 1430, 1337, 1280, 1169, 1038, 995, 884, 855, 812, 757, 724 cm^{-1} ; $^1\text{H NMR}$ (Acetone- d_6) δ 8.63 (s, 1H, aromatic proton), 5.14 (t, $^3J= 5.6\text{Hz}$, 2H, methylene protons), 5.08 (t, $^3J= 4.8\text{Hz}$, 2H, methylene protons), 5.02 (s, 2H, methylene protons), 2.55 (s, 3H, methyl protons); MS (APCI $^+$) m/z 297 (M^+).

Synthesis of 6-amino-4-imino-1-(2-hydroxyethyl)-2-hydroxymethyl-5-methyl-1*H*-benzimidazole-7-one (6). 100mg (0.00025 moles) of 5 was dissolved in a minimum amount of methanol and reduced under 50 psi of H_2 in the presence of 60mg of 5% Pd on carbon for 24 h. The catalyst was then filtered off using Celite as a filtering aid. The methanol was removed under reduced pressure and the resulting clear oil was dissolved in 20mL of dibasic phosphate buffer (pH=7). 208mg (0.00078 moles) of Fremy salt (potassium nitrosodisulfonate) was added

to the solution turning the previously clear buffer into a deep purple. This solution was stirred at room temperature for 0.5 h and was then loaded directly onto a C18 reverse phase column. Once loaded the column, water was used to elute remaining buffers and salts. The eluent was then changed to methanol, once the purple band was halfway down the column, a few drops of concentrated HCl was added to the methanol eluent. The purple band was collected and stripped of solvent under reduced pressure. The resulting purple oil was then dissolved using a few drops of ethanol, and crystallized by triturating with ethyl acetate. 16mg (0.055 mmoles) of the purple solid was filtered off as the HCl salt, compound 6 (22% yield); mp dec>140°C; TLC (n-Butanol/Acetic Acid/H₂O 5:2:3) R_f=0.41; IR (KBr Pellet) 3422, 3147, 1626, 1508, 1068, 978, 885, 707 cm⁻¹; ¹H NMR (Methanol- *d*₄) δ 4.66 (s, 2H, methylene protons), 4.44 (t, ³J= 5Hz, 2H, methylene protons), 3.68 (t, ³J= 5.2Hz, 2H, methylene protons), 1.93 (s, 3H, methyl protons); MS (APCI⁺) m/z 251 (M⁺).

Synthesis of 6-amino-2-chloromethyl-4-imino-1-(2-methanesulfonyethyl)-5-methyl-1*H*-benzimidazole-7-one (1A). 100mg (0.35 mmoles) of 6 was dissolved in dry pyridine and cooled on an ice bath. 80mg (0.7mmoles) of methanesulfonyl chloride was slowly added to the solution. After 45 minutes of stirring, the pyridine was removed under reduced pressure. The resulting oil was washed with chloroform and decanted to remove any remaining pyridine. The purple solid was then dissolved in a minimum amount of water and loaded onto a C18 reverse phase column. The column was washed in a gradient of 100% H₂O to 100% methanol. The purple product was washed off the column

using 0.1N HCl, the solvent was then removed under reduced pressure. The resulting purple oil was dissolved in a minimum amount of methanol and crystallized by trituration with a minimum amount of hexanes. This solution was centrifuged down into a pellet and decanted of solvent. The pellet was then suspended in acetone and sonicated, this was then centrifuged down to a pellet and the solvent was decanted. The remaining purple solid was dried under reduced pressure resulting in 30mg (0.08 mmole) of compound 1A (23% yield); mp dec>149°C; TLC (n-Butanol/Acetic Acid/H₂O 5:2:3) R_f=0.27; IR (KBr Pellet) 1626, 1510, 1347, 1173, 1014, 978, 919 cm⁻¹; ¹H NMR (Methanol- *d*₄) δ 5.00 (s, 2H, methylene protons), 4.70 (t, ³J= 5Hz, 2H, methylene protons), 4.54 (t, ³J= 5.2Hz, 2H, methylene protons), 3.14 (s, 3H, sulfonyl methyl protons), 1.93 (s, 3H, methyl protons); MS (APCI⁺) m/z 347 (M⁺).

Synthesis of 5-methyl-1-(2-oxyethyl)-2-oxypropyl-benzimidazole (7). A suspension of 5g (0.025 moles) of 3 was suspended in 150ml of 4N HCl and reduced under 50 psi of H₂ in the presence of 100mg of 5% Pd on carbon for 24 h. The catalyst was then filtered off using Celite as a filtering aid. 4.3g (0.050 moles) of gamma-butyrolactone (GBL) was added to the filtrate, the resulting solution was then refluxed for one hour. The reaction was first cooled to room temperature, and then place on an ice bath and made basic (pH=10) using ammonium hydroxide. The resulting solution was extracted 3x with chloroform and dried over sodium sulfate. The solvent was removed under reduced pressure and the remaining clear oil was scratched with a glass stir rod to induce crystallization. The white solid was recrystallized in ethanol to give 5.0g of

compound **7** (84% yield); mp 135-138°C; TLC (Chloroform/Methanol (90:10)) $R_f=0.49$; $^1\text{H NMR}$ (CDCl_3) δ 7.19 (s, 1H, aromatic proton), 7.13 (d, $^3J= 8\text{Hz}$, 1H, aromatic proton), 6.99 (dd, $^3J= 8.4\text{Hz}$, 1H, aromatic proton), 4.21 (t, $^3J= 5.2\text{Hz}$, 2H, methylene protons), 3.19 (t, $^3J= 5.2\text{Hz}$, 2H, methylene protons), 3.59 (t, $^3J= 5.4\text{Hz}$, 2H, methylene protons), 2.99 (t, $^3J= 6.8\text{Hz}$, 2H, methylene protons), 2.33 (s, 3H, methyl protons), 1.97 (m, 2H, methylene protons).

Synthesis of 4,6-dinitro-5-methyl-1-(2-nitrooxyethyl)-2-nitrooxypropyl-*1H*-benzimidazole (**8**). 0.55g (0.0023 moles) of **7** was dissolved in a minimal amount of concentrated sulfuric acid, this solution was then set on an ice bath and cooled to 0°C. 0.59g (0.0094 moles) of 90% fuming nitric acid was added to the solution drop wise while paying careful attention to not allow the temperature to rise above 10°C. Once the addition was complete, the solution was stirred at 50°C for 24 h till one spot remained on TLC. This solution was then neutralized with saturated sodium bicarbonate (pH=8) and extracted 3x with ethyl acetate. The organic solvent was then removed under reduced pressure to give a pale yellow oil. A flash silica column using ethyl acetate as the eluent was used to remove origin spots that remained on the TLC, it was common for new spots on the TLC to form after work up, these compounds were characterized and found to be the hydrolysis products of the nitrate esters. The ethyl acetate was removed under reduced pressure to give a pale oil that was recrystallized in ethanol to give 0.44g of compound **8** (59% yield) as a white crystal; mp 109-110°C; TLC (Ethyl acetate) $R_f=0.74$; $^1\text{H NMR}$ ($\text{DMSO}-d_6$) 7.70 (s, 1H, aromatic proton), 3.83 (t, $^3J= 5\text{Hz}$, 2H, methylene protons), 3.76 (t, $^3J= 5\text{Hz}$, 2H, methylene protons), 3.64 (t,

$^3J= 6.4\text{Hz}$, 2H, methylene protons), 2.06 (t, $^3J= 7.4\text{Hz}$, 2H, methylene protons), 1.43 (s, 3H, methyl protons), 1.21 (m, 2H, methylene protons).

Synthesis of 6-amino-4-imino-1-(2-hydroxyethyl)-2-hydroxypropyl-5-methyl-1*H*-benzimidazole-7-one (9). 200mg (0.48 mmoles) of 8 was dissolved in a minimum amount of methanol and reduced under 50 psi of H_2 in the presence of 50mg of 5% Pd on carbon for 24 h. The catalyst was then filtered off using Celite as a filtering aid. The methanol was removed under reduced pressure and the resulting clear oil was dissolved in 20mL of dibasic phosphate buffer (pH=7). 388mg (1.45 mmoles) of Fremy salt (potassium nitrosodisulfonate) was added to the solution turning the previously clear buffer into a deep purple. This solution was stirred at room temperature for 0.5 h and was then loaded directly onto a C18 reverse phase column. Once loaded the column, water was used to elute remaining buffers and salts. The eluent was then changed to methanol, once the purple band was halfway down the column, a few drops of concentrated HCl was added to the methanol eluent. The purple band was collected and stripped of solvent under reduced pressure. The resulting purple oil was then dissolved using a few drops of ethanol, and crystallized by triturating with ethyl acetate. 130mg (0.41 mmoles) of the purple solid was filtered off as the HCl salt, compound 9 (87% yield); mp dec>146°C; TLC (n-Butanol/Acetic Acid/ H_2O 5:2:3) $R_f=0.35$; ^1H NMR ($\text{DMSO-}d_6$) δ 4.99 (t, $^3J= 5.6\text{Hz}$, 2H, methylene protons), 4.58 (t, $^3J= 5\text{Hz}$, 2H, methylene protons), 4.25 (t, $^3J= 5\text{Hz}$, 2H, methylene protons), 3.64 (q, $^3J= 5.3\text{Hz}$, 2H, methylene protons), 3.45 (t, $^3J= 6\text{Hz}$, 2H, methylene protons), 2.84 (t,

$^3J = 7.6\text{Hz}$, 2H, methylene protons), 1.89 (s, 3H, methyl protons), 1.85 (m, 2H, methylene protons).

Synthesis of 6-amino-2-hydroxypropyl-4-imino-1-(2-methansulfonyethyl)-5-methyl-*IH*-benzimidazole-7-one (1B) and 6-amino-4-imino-1-(2-methansulfonyethyl)-2-methansulfonypropyl-5-methyl-*IH*-benzimidazole-7-one (1C). 71mg (0.23 mmoles) of 9 was dissolved in dry pyridine and cooled on an ice bath. 52mg (0.46mmoles) of methanesulfonyl chloride was slowly added to the solution. After 30 minutes of stirring, the pyridine was removed under reduced pressure. The resulting oil was washed with chloroform and decanted to remove any remaining pyridine. The purple solid was then dissolved in a minimum amount of water and loaded onto a C18 reverse phase column. The column was washed in a gradient of 100% H₂O to 100% methanol. Two purple bands separated on the column and were isolated separately when washed off using 1N HCl. The two fractions in question were worked up in similar fashion. The solvent was first removed under reduced pressure. The resulting purple oil was then dissolved in a minimum amount of methanol and crystallized by trituration with a minimum amount of hexanes. This solution was centrifuged down into a pellet and decanted of solvent. The pellet was then suspended in acetone and sonicated followed by centrifugation. The solvent was decanted from each of the two samples prepared. Each purple solid was separately dried under reduced pressure resulting in 15mg (0.037 mmoles) of the monosulfonated compound 1B (17% yield); mp dec>137°C; TLC (n-Butanol/Acetic Acid/H₂O 5:2:3) R_f=0.36; ¹H NMR (Methanol- *d*₄) δ 4.68 (t, $^3J =$

3.6Hz, 2H, methylene protons), 4.61 (t, $^3J= 3.8\text{Hz}$, 2H, methylene protons), 3.77 (t, $^3J= 6.4\text{Hz}$, 2H, methylene protons), 3.07 (s, 3H, sulfonyl methyl protons), 3.05 (t, $^3J= 7.6\text{Hz}$, 2H, methylene protons), 2.34 (s, 2H, methylene protons), 1.99 (s, 3H, methyl protons) and 10mg (0.021 mmoles) di-sulfonated compound 1C (9% yield); mp dec>143°C; TLC (n-Butanol/Acetic Acid/H₂O 5:2:3) R_f=0.61; ¹H NMR (DMSO- *d*₆) δ 10.07 (s, 1H, iminium proton), 9.84 (s, 1H, iminium proton), 8.68 (s, 2H, amine protons), 4.58 (t, $^3J= 4.6\text{Hz}$, 2H, methylene protons), 4.49 (t, $^3J= 4.4\text{Hz}$, 2H, methylene protons), 3.77 (t, $^3J= 6.4\text{Hz}$, 2H, methylene protons), 3.11 (s, 3H, sulfonyl methyl protons), 2.93 (t, $^3J= 7.4\text{Hz}$, 2H, methylene protons), 2.23 (s, 3H, sulfonyl methyl protons), 2.19 (m, 2H, methylene protons), 1.89 (s, 3H, methyl protons).

Synthesis of 1-(2-Hydroxyethyl)-5-methylbenzimidazole (10). A suspension of 0.5g (0.0025 moles) of 3 was suspended in 50ml of 4N HCl and reduced under 50 psi of H₂ in the presence of 50mg of 5% Pd on carbon for 24 h. The catalyst was then filtered off using Celite as a filtering aid. 0.1g (0.0050 moles) of 96% formic acid was added to the filtrate, the resulting solution was then refluxed for one hour. The reaction was first cooled to room temperature, and then placed on an ice bath and made basic (pH=10) using ammonium hydroxide. The white precipitate was filtered and rinsed with cold water to give 0.36g (0.024 moles) of compound 10 (81% yield); mp 134-136°C; TLC (Chloroform/Methanol (90:10)) R_f=0.40; IR (KBr pellet) 790, 869, 1076, 1178, 1253, 1329, 1386, 1510, 1780, 2868, 3090, 3171, cm⁻¹; ¹H NMR (CDCl₃) δ 7.18 (d, $^3J= 8\text{Hz}$, 1H, aromatic proton), 7.11 (s, 1H, aromatic proton), 7.03 (d, $J= 8\text{Hz}$, 1H, aromatic proton),

4.26 (t, $J = 5\text{Hz}$, 2H, methylene protons), 4.04 (t, $J = 5\text{Hz}$, 2H, methylene protons), 2.35 (s, 3H, methyl protons).

Synthesis of 4,6-dinitro-5-methyl-1-(2-nitrooxyethyl)-*1H*-benzimidazole (11). 1g (0.0048 moles) of 11 was dissolved in a minimal amount of concentrated sulfuric acid, this solution was then set on an ice bath and cooled to 0°C. 0.92g (0.0145 moles) of 90% fuming nitric acid was added to the solution drop wise while paying careful attention to not allow the temperature to rise above 10°C. Once the addition was complete, the solution was stirred at 50°C for 24 h till one spot remained on TLC. This solution was then neutralized with saturated sodium bicarbonate (pH=8) and extracted 3x with ethyl acetate. The organic solvent was then removed under reduced pressure to give a clear oil. A flash silica column using ethyl acetate as the eluent was used to remove origin spots that remained on the TLC. The ethyl acetate was removed under reduced pressure to give a clear oil that was recrystallized in ethanol to give 1.3g (0.0042 moles) of compound 11 (86% yield) as a white crystal; mp 130-131°C; TLC (Ethyl acetate) $R_f=0.43$. ^1H NMR (Acetone- d_6) δ 8.69 (s, 1H, imidazole proton), 8.62 (s, 1H, aromatic proton), 5.09 (t, $J = 5\text{Hz}$, 2H, methylene protons), 5.03 (t, $J = 5\text{Hz}$, 2H, methylene protons), 2.53 (s, 3H, methyl protons).

Synthesis of 6-amino-4-imino-1-(2-hydroxyethyl)-5-methyl-*1H*-benzimidazole-7-one (12). 200mg (0.64 mmoles) of 11 was dissolved in a minimum amount of methanol and reduced under 50 psi of H_2 in the presence of 50mg of 5% Pd on carbon for 24 h. The catalyst was then filtered off using Celite as a filtering aid. The methanol was removed under reduced pressure and the

resulting clear oil was dissolved in 20mL of dibasic phosphate buffer (pH=7). 0.52g (1.9 mmoles) of Fremy salt (potassium nitrosodisulfonate) was added to the solution turning the previously clear buffer into a deep purple. This solution was stirred at room temperature for 0.5 h and was then loaded directly onto a C18 reverse phase column. Once loaded the column, water was used to elute remaining buffers and salts. The eluent was then changed to methanol, once the purple band was halfway down the column, a few drops of concentrated HCl was added to the methanol eluent. The purple band was collected and stripped of solvent under reduced pressure. The resulting purple oil was then dissolved using a few drops of ethanol, and crystallized by triturating with ethyl acetate. 132mg (0.51 mmoles) of the purple solid was filtered off as the HCl salt, compound 12 (80% yield); mp dec>145°C; TLC (n-Butanol/Acetic Acid/H₂O 5:2:3) R_f=0.44.

Synthesis of 6-amino-4-imino-1-(2-methanesulfonyethyl)-5-methyl-1*H*-benzimidazole-7-one (1D). 40mg (0.16 mmoles) of 12 was dissolved in dry pyridine and cooled on an ice bath. 35.7mg (0.31 mmoles) of methanesulfonyl chloride was slowly added to the solution. After 1 h of stirring, the pyridine was removed under reduced pressure. The resulting oil was washed with chloroform and decanted to remove any remaining pyridine. The purple solid was then dissolved in a minimum amount of water and loaded onto a C18 reverse phase column. The column was washed in a gradient of 100% H₂O to 100% methanol. The purple product was washed off the column using 1N HCl, the solvent was then removed under reduced pressure. The resulting purple oil was dissolved in a minimum amount of methanol and crystallized by trituration with a minimum

amount of hexanes. This solution was centrifuged down into a pellet and decanted of solvent. The pellet was then suspended in acetone and sonicated, this was then centrifuged down to a pellet and the solvent was decanted. The remaining purple solid was dried under reduced pressure resulting in 26mg (0.08 mmole) of compound 1D (50% yield); mp dec>135°C; TLC (n-Butanol/Acetic Acid/H₂O 5:2:3) R_f=0.40; ¹H NMR (DMSO- *d*₆) δ 4.63 (t, ³J= 4.8Hz, 2H, methylene protons), 4.57 (t, ³J= 5.2Hz, 2H, methylene protons), 3.04 (s, 3H, sulfonyl methyl protons), 1.99 (s, 3H, methyl protons).

Synthesis of N,3-dimethyl-2-aminoaniline (14). Compound 14 synthesized as previously reported (Ahn, Kim, & Han, 1998). Concentrated HCl was added drop wise to 1g (0.0060 moles) of 13 while on an ice bath. 0.5 g of finely divided Zn was slowly added to the reaction until the solution turned from red to clear. At this point 50 ml of cold H₂O was added and the solution was filtered to remove excess zinc. This filtrate was carefully neutralized using sodium bicarbonate (pH=8) and immediately extracted 2x with ethyl acetate. The organic phase was then treated with two drops of concentrated sulfuric acid to precipitate the diamine salt 14. This product was filtered and washed with cold ethyl acetate to give 1.1g (0.0047 moles) of compound 14 (77% yield); mp 123-125°C; TLC (Chloroform/ Methanol (90:10)) R_f=0.02; IR (KBr) 3388, 3079, 2919, 1638, 1571, 1526, 1512, 1393, 1352, 1273, 1222, 1177, 1051 cm⁻¹; ¹H NMR (DMSO- *d*₆) δ 8.06 (s, 1H, amine proton), 7.86-6.89 (m, 3H, aromatic protons), 3.31 (s, 3H, N-methyl protons), 2.22 (s, 3H, methyl protons).

Synthesis of 1,5-dimethyl-1*H*-benzimidazole-2-methanamine (15).

Compound 3 synthesized as previously reported (Cariou, Gibson, Tomov, & White, 2009). 0.5g (0.0021 moles) of 14 was dissolved in 15ml of 6N HCl. 0.16g (0.0021 moles) of glycine was added to this solution and refluxed for 24hr. This was then momentarily boiled over activated charcoal and then filtered. The filtrate was removed under reduced pressure resulting in a blue crystalline solid. This solid was recrystallized in ethanol to give 0.37g (0.0017 moles) of 15 (83% yield); mp 140-142°C; TLC (n-Butanol/Acetic Acid/H₂O 5:2:3) R_f=0.45; ¹H NMR (D₂O) δ 7.84 (m, 2H, aromatic protons), 7.66 (m, 2H, aromatic protons), 4.09 (s, 3H, N-methyl protons).

REFERENCES

- Ahn, C. M., Kim, S. K., & Han, J. L. (1998). Synthesis of 6-aziridinylbenzimidazole derivatives and their in vitro antitumor activities. *Archives of Pharmacal Research*, 21(5), 599-609.
- American Cancer Society. *Breast Cancer Facts & Figures 2009-2010*. Atlanta: American Cancer Society, Inc.
- American Cancer Society. (20). *Cancer facts & figures 2010*. American Cancer Society.
- Anslyn, E. V., & Dougherty, D. A. (2006). *Modern Physical Organic Chemistry*. Sausalito, Calif.: University Science.
- Baguley, B. C., & Kerr, D. J. (2002). *Anticancer drug development*. San Diego, Calif.; London: Academic.
- Barnhill, R. L. (1995). *Pathology of Melanocytic Nevi and Malignant Melanoma*. Boston, MA: Butterworth-Heinemann.
- Berger, A., Quast, S., Plötz, M., Hein, M., Kunz, M., Langer, P., & Eberle, J. (2011). Sensitization of melanoma cells for death ligand-induced apoptosis by an indirubin derivative—Enhancement of both extrinsic and intrinsic apoptosis pathways. *Biochemical Pharmacology*, 81(1), 71-81.
- Boyd, M. R., & Paull, K. D. (1995). Some practical considerations and applications of the national cancer institute in vitro anticancer drug discovery screen. *Drug Development Research*, 34(2), 91-109.
- Cariou, R., Gibson, V. C., Tomov, A. K., & White, A. J. P. (2009). Group 4 metal complexes bearing new tridentate (NNO) ligands: Benzyl migration and formation of unusual CC coupled products. *Journal of Organometallic Chemistry*, 694(5), 703-716.
- Carney, J. R., Scheuer, P. J., & Kelly-Borges, M. (1993). Makaluvamine G, a cytotoxic pigment from an Indonesian sponge *Heterodermella* sp. *Tetrahedron*, 49(38), 8483-8486.
- Chao, D. T., & Korsmeyer, S. J. (1998). BCL-2 FAMILY: Regulators of cell death. *Annual Review of Immunology*, 16(1), 395.

- Cohen, M. S., Zhang, C., Shokat, K. M., & Taunton, J. (2005). Structural bioinformatics-based design of selective, irreversible kinase inhibitors. *Science*, 308(5726), 1318.
- Copp, B. R., Ireland, C. M., & Barrows, L. R. (1991). Wakayin: A novel cytotoxic pyrroloiminoquinone alkaloid from the ascidian clavelina species. *The Journal of Organic Chemistry*, 56(15), 4596-4597.
- DeVita, V. T., & Chu, E. (2008). A history of cancer chemotherapy. *Cancer Research*, 68(21), 8643.
- Hanks, S. K., Quinn, A. M., & Hunter, T. (1988). The protein kinase family: Conserved features and deduced phylogeny of the catalytic domains. *Science*, 241(4861), 42.
- Henshall, D. C., Araki, T., Schindler, C. K., Lan, J. Q., Tiekoter, K. L., Taki, W., & Simon, R. P. (2002). Activation of bcl-2-associated death protein and counter-response of akt within cell populations during seizure-induced neuronal death. *Journal of Neuroscience*, 22(19), 8458.
- Herlyn, M. (1993). *Molecular and Cellular Biology of Melanoma*. Austin: R.G. Landes Co.
- Hickman, J. A., & Tritton, T. R. (1993). *Cancer Chemotherapy*. Oxford England; Boston: Blackwell Scientific Publications.
- Hoang, H., LaBarbera, D. V., Mohammed, K. A., Chris, M., & Skibo, E. B. (2007). Synthesis and biological evaluation of imidazoquinoxalinones, imidazole analogues of pyrroloiminoquinone marine natural products. *Journal of Medicinal Chemistry*, 50(19), 4561-4571.
- Hocker, T., & Tsao, H. (2007). Ultraviolet radiation and melanoma: A systematic review and analysis of reported sequence variants. *Human Mutation*, 28(6), 578-588.
- Kitada, S., Krajewska, M., Zhang, X., Scudiero, D., Zapata, J. M., Wang, H. G., . . . Reed, J. C. (1998). Expression and location of pro-apoptotic bcl-2 family protein BAD in normal human tissues and tumor cell lines. *The American Journal of Pathology*, 152(1), 51-61.
- Knight, Z. A., & Shokat, K. M. (2005). Features of selective kinase inhibitors. *Chemistry & Biology*, 12(6), 621-637.

- LaBarbera, D. V., & Skibo, E. B. (2005). Synthesis of imidazo[1,5,4-de]quinoxalin-9-ones, benzimidazole analogues of pyrroloiminoquinone marine natural products. *Bioorganic & Medicinal Chemistry*, *13*(2), 387-395.
- Li, W., Zhou, J., Chen, L., Luo, Z., & Zhao, Y. (2011). Lysyl oxidase, A critical intra-and extra-cellular target in the lung for cigarette smoke pathogenesis. *International Journal of Environmental Research and Public Health*, *8*(1), 161.
- Lopez-Bergami, P., & Fitchman, B. (2008). Understanding signaling cascades in melanoma. *Photochemistry and Photobiology*, *84*(2), 289.
- Nguyen, T. L., Gussio, R., Smith, J. A., Lannigan, D. A., Hecht, S. M., Scudiero, D. A., . . . Zaharevitz, D. W. (2006). Homology model of RSK2 N-terminal kinase domain, structure-based identification of novel RSK2 inhibitors, and preliminary common pharmacophore. *Bioorganic & Medicinal Chemistry*, *14*(17), 6097-6105.
- Puissant, A., Robert, G., Fenouille, N., Luciano, F., Cassuto, J. P., Raynaud, S., & Auberger, P. (2010). Resveratrol promotes autophagic cell death in chronic myelogenous leukemia cells via JNK-mediated p62/SQSTM1 expression and AMPK activation. *Cancer Research*, *70*(3), 1042.
- Qin, J., Xin, H., Sitailo, L. A., Denning, M. F., & Nickoloff, B. J. (2006). Enhanced killing of melanoma cells by simultaneously targeting mcl-1 and NOXA. *Cancer Research*, *66*(19), 9636-9645.
- Rümke, P. (1990). *Therapy of advanced melanoma*. Basel; New York: Karger.
- Reed, J. C. (1994). Bcl-2 and the regulation of programmed cell death. *The Journal of Cell Biology*, *124*(1), 1.
- Shukla, S., Bharti, A. C., Mahata, S., Hussain, S., Kumar, R., Hedau, S., & Das, B. C. (2009). Infection of human papillomaviruses in cancers of different human organ sites. *Indian Journal of Medical Research*, *130*(3), 222-233.
- Trosko, J. E. (2003). The role of stem cells and gap junctional intercellular communication in carcinogenesis. *Journal of Biochemistry and Molecular Biology*, *36*(1), 43-48.
- Wilson, C. O., Gisvold, O., Block, J. H., & Beale, J. M. (2004). *Wilson and Gisvold's Textbook of Organic Medicinal and Pharmaceutical Chemistry* (11th ed.). Philadelphia; London: Lippincott Williams & Wilkins.